Binary nucleation of sulfuric acid-water: Monte Carlo simulation

I. Kusaka, Z.-G. Wang, and J. H. Seinfeld
Department of Chemical Engineering, California Institute of Technology, Pasadena, California 91125

We have developed a classical mechanical model for the H_2SO_4/H_2O binary system. Monte Carlo simulation was performed in a mixed ensemble, in which the number of sulfuric acid molecules is fixed while that of water molecules is allowed to fluctuate. Simulation in this ensemble is computationally efficient compared to conventional canonical simulation, both in sampling very different configurations of clusters relevant in nucleation and in evaluating the free energy of cluster formation. The simulation yields molecular level information, such as the shape of the clusters and the dissociation behavior of the acid molecule in the cluster. Our results indicate that the clusters are highly nonspherical as a result of the anisotropic intermolecular interactions and that a cluster with a given number of acid molecules has several very different conformations, which are close in free energy and hence equally relevant in nucleation. The dissociation behavior of H_2SO_4 in a cluster differs markedly from that in bulk solution and depends sensitively on the assumed value of the free energy f_{hb} of the dissociation reaction $H_2SO_4 + H_2O \rightarrow HSO_4^- \cdot H_3O^+$. In a small cluster, no dissociation is observed. As the cluster size becomes larger, the probability of having an $HSO_4^- \cdot H_3O^+$ ion pair increases. However, in clusters relevant in nucleation, the resulting ion pairs remain in contact; about 240 water molecules are required to observe behavior that resembles that in bulk solution. If a larger value of f_{hb} is assumed to reflect its uncertainty, the probability of dissociation becomes negligible. A reversible work surface obtained for a condition typical of vapor to liquid nucleation suggests that the rate-limiting step of new particle formation is a binary collision of two hydrated sulfuric acid molecules. The ion pairs formed by dissociation play a key role in stabilizing the resulting cluster. The reversible work surface is sensitive to the assumed value of f_{hb}, thus pointing to the need for an accurate estimate of the quantity either by *ab initio* calculations or experiments. © *1998 American Institute of Physics.* [S0021-9606(98)51716-3]

I. INTRODUCTION

The theory of binary nucleation dates back to a paper by Reiss.[1] Despite successive modification accounting for transient behaviors and paths in the vicinity of the saddle point,[2–7] the theory is an extension of the classical nucleation theory for single component systems. While the classical theory[8–10] is presently the only practical approach for predicting nucleation rates, limitations of the theory, arising from its macroscopic nature, are well known. Thus, there has been a great interest in establishing molecular level approaches to nucleation.

One of the most important binary nucleating systems is H_2SO_4/H_2O, to which numerous papers are devoted on both theoretical[11–26] and experimental[27–32] fronts. Comparisons of the classical predictions with experimental data for H_2SO_4/H_2O nucleation, while not extensive, yield conflicting results as to the validity of the classical theory.[19,28,29,31,32] Thus, it is of great interest on both fundamental and practical grounds, to seek a molecular level description of binary H_2SO_4/H_2O nucleation.

There are two major trends in developing a molecular level theory of nucleation. One is a molecular level simulation,[33–41] which can be applied regardless of the complexity of the intermolecular interaction. However, the free energy of a cluster, the quantity of central importance in nucleation theory, is usually evaluated by integrating its internal energy obtained at different temperatures from separate simulations. This aspect renders the approach computationally demanding and, as a result, virtually all of the simulations are limited to a single component system. The alternative approach is to use statistical mechanical density functional theory,[42] first applied to homogeneous nucleation by Oxtoby and Evans.[43] In this approach, the grand potential of the system is written as a functional of order parameters. Then, the stationarity condition of the grand potential determines the order parameters for the critical nucleus and the corresponding grand potential follows from the functional. When a cluster possesses a high degree of symmetry and the intermolecular potential is relatively simple, this approach is computationally far less demanding, allowing one to investigate a much wider range of the parameter space. Thus, one usually employs model potentials that capture the essential features of the molecules under consideration. When the results are compared against predictions from the classical theory, which uses bulk thermodynamic quantities obtained from the same theoretical framework, one can isolate the deviations from the classical predictions arising from the molecular level details. Although the approach is more approximate compared to molecular simulation, the theory is extremely powerful in addressing the deviations in a semi-quantitative manner and has been employed to investigate several interesting systems[44–52] for which no simulation has

been performed. The theory was recently applied to a ternary system.[53]

In the present case of the H_2SO_4/H_2O binary system, however, density functional theory does not offer any advantage over simulation, for the intermolecular potentials that can faithfully represent the system are very complicated and as a result of the strongly anisotropic intermolecular interactions, a small cluster is expected to be highly non-spherical. Consequently, we resort to a method of computer simulation, in particular Monte Carlo simulation, since we are primarily concerned with equilibrium properties of the clusters. To our knowledge, the present work is the first example in which an extensive evaluation is made of the free energy of cluster formation in a binary system. The lack of a simulation in a binary system is a result of the extensive computation involved in the free energy calculation. Thus, one of our goals in the present work is to establish a simulation technique that considerably reduces the computational effort.

The intermolecular interaction potential is the fundamental information prerequisite in applying a molecular theory. To reproduce this potential in a simple way, one usually represents a molecule as a set of interaction sites rigidly held together in its representative geometry. The interaction parameters are then optimized to reproduce *ab initio* results for geometries and energies of small clusters or certain bulk thermodynamic properties. The main concern in this approach is the quality of the potential thus obtained. For example, the necessity of incorporating molecular polarizabilities or three-body potentials in accurately reproducing the energy and the geometry of a cluster is often stressed.[54,55] In the case of a cluster of highly associative molecules, however, simulation must be performed for a very long period of time to sample faithfully the relevant parts of the phase space. For a water cluster, for example, this is necessary because the strong intermolecular interaction arising from an extensive hydrogen bond network hinders the evolution of the cluster from one structure to another, even though very different structures have to be taken into account in evaluating the thermodynamic properties of the cluster. In the present case of the H_2SO_4/H_2O system, even stronger hydrogen bonds are expected to be involved,[56] as is suggested by the relatively high boiling point of the pure acid (330 °C). Thus, in order to perform a feasible calculation to obtain the free energy of the clusters, we must be content with simple model potentials.

Nonetheless, simulation provides significant molecular level insight that is otherwise unattainable. Since the size of a typical cluster, containing a few acid molecules and several tens of water molecules, is smaller than the Bjerrum length, the distance at which the Coulombic interaction of a pair of ions becomes comparable with the thermal energy, the dissociation behavior of a sulfuric acid molecule in the cluster can be quite different from that in bulk solution. In the classical nucleation theory, however, the reversible work of cluster formation is expressed in terms of bulk thermodynamic quantities. It follows that the reversible work estimated by the classical theory may not reflect the true dissociation behavior in the cluster, whose effect can be addressed only by a molecular approach. Another conceptually, if not quantita-

tively, important problem relates to the very foundation of the thermodynamics of interfaces. Unless a cluster is spherical on average, the formalism loses its validity as the thickness of the interfacial region becomes non-negligible compared to the size of the cluster itself.[57] As mentioned above, however, a small cluster is expected to be highly non-spherical even after a thermal average is taken.

Given the limitations on the quality of the intermolecular potentials, a sensible way to address the effect of the molecular level details is to compare the results from simulation with the classical predictions obtained by using bulk thermodynamic properties for the system with the same model potentials used in simulation. Computation involved in determining these properties from simulation with the required accuracy is demanding and beyond the scope of this work. Instead, we shall directly compare the reversible work surface from simulation with the classical predictions for a real H_2SO_4/H_2O system.

This paper is organized as follows. The model potential is developed in Sec. II. In Sec. III, we derive the expression for the reversible work of cluster formation. In this section we employ a mixed ensemble, in which the number of water molecules is allowed to fluctuate while that of acid molecules is fixed. As a result, a cluster is characterized solely by the number of acid molecules inside it. In Sec. IV, we characterize a cluster by the numbers of molecules of both water and acid and derive the expressions for the reversible work and the equilibrium distribution for this cluster. The resulting expressions can be readily evaluated from the results of the mixed ensemble simulation. Section V describes certain details of the simulation. Results of simulation are presented in Sec. VI, where a comparison is made between the reversible work from molecular simulation and that from the classical theory. The paper concludes in Sec. VII with a brief discussion on the implications of our work.

II. MODEL

Given the possibility of dissociation and protonation of the molecules involved, conceptually the simplest approach is to represent the H_2SO_4/H_2O system as a mixture of reactive species of water, sulfate ion, and proton. In the initial stage of this work, we investigated this possibility[58] and encountered serious difficulties. Briefly, to take advantage of the existing models for water[59] and sulfate ion,[60] a proton was described as a unit charge $|e|$, where e is the charge of an electron, with Lennard-Jones parameters that reproduce O-H bond energies of hydronium ion and sulfuric acid. Since both bond energies are of the order of 10^2 kcal/mol, however, protons rarely change their positions during a simulation. Consequently, the system becomes locked into a local minimum dictated mainly by the initial configuration of protons. This behavior is in serious contradiction with the experimental value of the activation energy for proton transfer in water, which is estimated to be about a few kcal/mol.[61,62]

An alternative model was proposed by Hale and Kathmann,[63] in which a partial charge less than $|e|$ is assigned to a proton. Although the model cannot describe either dissociation of acid or protonation of water, and hence is inapplicable for the present purpose of addressing the disso-

ciation behavior in a cluster, it can explicitly incorporate internal rotations and vibrations of O-H bonds in a sulfuric acid molecule. Such internal degrees of freedom can be important. In a $H_2SO_4 \cdot H_2O$ dimer in vacuum, for example, the potential energy barrier for internal rotation of the O-H bonds of the acid molecule is estimated to be 5.2 kcal/mol by *ab initio* calculation at the MP2/3-21g** level of theory,[64] suggesting a possibility of more than one conformation of the dimer. Some of these conformations become unavailable to the dimer as it is transferred from the vapor phase to the bulk liquid solution simply because of the dissociation of the acid molecule. This indicates that the contribution to the dimer free energy from certain conformations is not included in the classical description which relies on bulk thermodynamic properties. Thus, the loss of an available conformation can contribute to an error in the classical free energy prediction.

Attempts to develop a dissociative model pose serious problems. Note that a proton in a dissociative model must carry a unit charge of $|e|$. In reality, however, its effective charge certainly is less than $|e|$, since a proton exists by forming a chemical bond to an oxygen from water or sulfate ion. Moreover, when one of the O-H bonds is broken and another is formed, the entire electronic structure of the molecules involved changes. This is inherently a quantum mechanical effect, which, when reproduced in the realm of classical mechanics, requires fairly detailed interaction potentials including explicit polarizabilities and three-body potentials, as illustrated by a dissociative model for pure water.[65,66] To develop a dissociative model for the present system, a substantial amount of data on energies and structures of sulfuric acid-water complexes is required. In this context, we note that the three-body potential can be quite sensitive to the exact environment. Thus, the dissociative model for pure water[65,66] is unlikely to remain valid in the present system. However, available literature dealing with such complexes is very limited. Apparently, only one such paper exists,[67] which provides interaction energies with partially optimized geometries of the neutral complex $H_2SO_4 \cdot H_2O$ and the ionic complex $HSO_4^- \cdot H_3O^+$. The lack of necessary information precludes an effort to develop a detailed interaction potential.

An *ab initio* molecular dynamics[68–71] approach, in which atomic nuclei are treated classical mechanically while the electronic degrees of freedom are treated explicitly by quantum mechanical density functional theory,[72] appears to be an interesting alternative. In this approach, no model potential needs to be specified, rather it is calculated on-the-fly during the course of simulation. However, its application is currently limited to investigating dynamics that occur on the time scale of the order of picoseconds and is not yet practical in evaluating free energy.

The approach adopted here is to treat the dissociated and undissociated states as distinct. Since a proton exists primarily as a part of either sulfuric acid or hydronium ion rather than as a free ion, and the second dissociation of sulfuric acid is negligible compared to the first, one can introduce water, hydronium ion, sulfuric acid, and bisulfate ion as the constituent molecules. A molecule is modeled as a set of interaction sites rigidly held together at a representative geom-

TABLE I. Interaction parameters for water and hydronium ion.

	Water	Hydronium ion
A_O^2 [kcal $Å^{12}$/mol]	0.62935×10^6	0.38931×10^6
C_O^2 [kcal $Å^6$/mol]	0.62545×10^3	0.65328×10^3
z_O	$-0.8476|e|$	$-0.2480|e|$
z_H	$0.4238|e|$	$0.4160|e|$
r(O-H) [Å]	1.000	0.973
$\angle$ H-O-H	109.47°	111.6°

etry. It is well known that nonadditive interactions, arising from molecular polarizabilities and three-body interactions, play an important role in both the energetics and the structures of clusters.[54,55] Nonetheless, the enormous computational effort involved in free energy calculation and the lack of either experimental or quantum mechanical data indicate one should adopt the simplest possible potential, namely a pairwise additive potential. Even then, in this four component system, there are as many as ten distinct interaction pairs, while the available data cover only four of them. For example, in addition to the data on the two complexes mentioned above, various water-water interaction potentials are available. Protonated water clusters have been a focus of extensive studies on both experimental[73–76] and theoretical[77–81] fronts. To estimate the remainder of the interactions, however, one needs to invoke some kind of mixing rule, which in turn requires that all of the pair interactions be described by the same type of function. In this work, the interaction potential $u_{\alpha\beta}$ between molecules α and β is assumed to be the sum of Coulombic and Lennard-Jones interactions,

$$u_{\alpha\beta} = \sum_{i \text{ on } \alpha} \sum_{j \text{ on } \beta} \left(\frac{z_i z_j}{r_{ij}} + \frac{A_i A_j}{r_{ij}^{12}} + \frac{C_i C_j}{r_{ij}^6} \right), \quad (1)$$

where r_{ij} is the distance between sites i and j and the summation is taken over all intermolecular interaction sites.

The model parameters are given in Tables I–III. The notations for the interaction sites for sulfuric acid and bisulfate ion are defined in Fig. 1. The geometries for these species are given in Table IV and discussed below. Parameters for water correspond to the SPC/E potential,[59] which is known to reproduce certain bulk properties of pure water including the coexistence densities[82] and the surface tension.[83,84] Parameters for the other molecules require explanation.

As mentioned above, protonated water clusters have been studied extensively and various interaction potentials have been proposed.[85–88] However, none assumes a form as simple as Eq. (1). Thus, it is necessary to develop a potential as follows. First, the geometry of the hydronium ion is taken

TABLE II. Lennard-Jones parameters of sulfuric acid molecule and bisulfate ion.

	Sulfur site	Oxygen sites
A_i^2 [kcal $Å^{12}$/mol]	0.40063×10^7	0.76351×10^6
C_i^2 [kcal $Å^6$/mol]	0.20016×10^4	0.78154×10^3

TABLE III. Partial charges on H_2SO_4 and HSO_4^-.

Interaction site	H_2SO_4	HSO_4^-
S	2.8528 $|e|$	2.8272 $|e|$
O_1	-1.0325 $|e|$	-1.2942 $|e|$
$O_{1'}$	-1.0325 $|e|$	-1.1482 $|e|$
O_2	-0.9582 $|e|$	-0.9615 $|e|$
$O_{2'}$	-0.9582 $|e|$	-0.9615 $|e|$
H_1	0.5643 $|e|$	$\cdots$
$H_{1'}$	0.5643 $|e|$	0.5382 $|e|$

TABLE IV. Sulfuric acid molecule geometry adopted in this work.

$r(O_1\text{-}H_1)$	0.97 Å
$r(\text{S-}O_1)$	1.574 Å
$r(\text{S}=O_2)$	1.422 Å
$\angle(H_1\text{-}O_1\text{-S})$	108.5°
$\angle(O_1\text{-S-}O_{1'})$	101.3°
$\angle(O_2=\text{S}=O_{2'})$	123.3°
$\tau(H_1O_1SO_2)$[a]	20.8°
$\tau(P_1P_2)$[b]	88.4°

[a]Looking down the O_1-S bond. The H_1O_1 projection must be rotated clockwise by 20.8° to be *cis* to the O_2-S bond.

[b]Angle between $O_1SO_{1'}$ and $O_2SO_{2'}$ planes. The small deviation from exactly perpendicular planes brings O_2 and $O_{2'}$ closer to $O_{1'}$ and O_1, respectively.

from the accurate theoretical determination by Rodwell and Radom.[89] Each atomic site bears a partial charge while the Lennard-Jones parameters are assigned only for the oxygen sites. Then, these parameters are tuned to reproduce the experimentally determined enthalpy of hydration of the ion hydrated up to six water molecules.[73] The difference between enthalpy and internal energy is ignored for simplicity. In parametrizing the partial charge on oxygen, either negative or positive charge can be assigned, yielding a similar overall agreement to the experimental enthalpy of hydration. However, the assignment of a negative charge resulted in interaction parameters that are closer to the values for SPC/E water and is preferred on the basis that the protonation of a molecule should not significantly change its interaction parameters. The resulting hydration energies are compared with experimental values in Table. V. Except for the first few hydrates, the agreement is fair.

The experimentally determined geometry is adopted for sulfuric acid[56] as shown in Fig. 1 and Table IV. A partially optimized geometry for bisulfate ion was obtained by Kurdi and Kochanski[67] using *ab initio* calculation. In their calculation, $\angle$ S-$O_{1'}$-$H_{1'}$=114° was obtained. However, the value is probably an overestimate insofar as the corresponding value for sulfuric acid was overestimated by 11.5°. In the present work, we simply use the same value as for sulfuric acid. We also ignore the slight ($\approx 0.5°$) deviation between the C_2 axes of the angle O_1-S-$O_{1'}$ and O_2=S=$O_{2'}$. In other words,

bisulfate ion was obtained from sulfuric acid by removing the proton H_1 and shortening the bond length $r(\text{S-}O_1)$ to 1.48 Å. In determining interaction parameters for these molecules, *ab initio* results[67] on the potential energies and geometries of $H_2SO_4\cdot H_2O$ and $HSO_4^-\cdot H_3O^+$ were used. The experimentally obtained dipole moment of sulfuric acid[56] provided additional information. The information, however, is simply not sufficiently extensive to determine all of the parameters. To further facilitate the parametrization, the Lennard-Jones parameters for these molecules were assumed to be the same as those of sulfate ion[60] and only the partial charges were adjusted. In addition, partial charges on O_2 and $O_{2'}$ sites of bisulfate ion are assumed to be equal, though these two sites are not equivalent. The resulting interaction energies and geometries are compared with the *ab initio* results in Tables VI and VII for sulfuric acid and bisulfate, respectively. In Table VI, other sets of *ab initio* results are shown. Judged from the level of the theory, the results by Morokuma and Muguruma[90] are perhaps the most accurate. Nonetheless, we employ the results by Kurdi and Kochanski[67] since the corresponding data for $HSO_4^-\cdot H_3O^+$ are available only in their paper. Because of some model parameters left unadjusted, the model is expected to be sufficiently flexible to incorporate additional data as they become available.

An iterative method similar to that suggested by Halley *et al.*[66] is used to find the optimum sets of parameters. First, simulation was carried out with some reasonable values of the parameters, for which the difference between the calculated and ''exact'' energies and structures of the complexes were evaluated. New sets of parameters were obtained by

FIG. 1. Model of a sulfuric acid molecule showing notations and C_2 axis.

TABLE V. Enthalpy of hydration from simulation and experimental values.

$n-1,n$	$-\Delta U_{n-1,n}$ [kcal/mol][a,b]	$-\Delta H_{n-1,n}$ [kcal/mol][a,c]
0,1	25.35	31.6
1,2	23.74	19.5
2,3	21.98	17.9
3,4	11.42	12.7
4,5	10.92	11.6
5,6	10.43	10.7

[a]$\Delta U_{n-1,n} \equiv U_n - U_{n-1}$, likewise for $\Delta H_{n-1,n}$.

[b]This work. Simulation performed at 298.15 K.

[c]Experimental data of Lau *et al.* (Ref. 73).

TABLE VI. Energy and geometry of $H_2SO_4 \cdot H_2O$ neutral complex. Comparison between simulation and ''exact'' values.

	This work[a]	Experiment[b]	Kurdi[c]	Morokuma[d]	Lay[e]
Energy [kcal/mol]	−15.76	⋯	−15.769	≈ -10.00	−25.37
O-O_1 distance [Å][f]	2.662	⋯	2.656	≈ 2.696	2.553
Dipole moment of H_2SO_4 [debye]	2.718	2.72515	⋯	⋯	2.2989

[a]Simulation was carried out at 0.1 K.
[b]Kuczkowski et al. (Ref. 56).
[c]Ab initio SCF-MO-LCGO calculation by Kurdi and Kochanski (Ref. 67).
[d]Ab initio calculation by Morokuma and Muguruma (Ref. 90) at the fourth-order MP4SDQ level with zero-point correction. The values cited here are estimated from their figures.
[e]Ab initio calculation by Lay (Ref. 64) at the MP2/3-21g** level.
[f]O is on water while O_1 is on sulfuric acid.

randomly perturbing the old parameters, which in turn were used to generate the next trial parameters only if they resulted in a decrease of the deviation. The process was repeated until no further decrease of the deviation is achieved.

III. REVERSIBLE WORK OF CLUSTER FORMATION

In this section, we derive a statistical mechanical expression for the reversible work of cluster formation from a H_2SO_4/H_2O binary vapor. Since the vapor phase serves as a reference state in calculating the reversible work, its precise nature has to be specified first. Most of the acid molecules in the vapor exist as hydrates so that the number of the sulfuric acid monomers is significantly smaller than the total number of acid molecules.[14,15,18,19,22,23,91] In deriving the statistical mechanical expression for the reversible work of cluster formation, it is most convenient to take a reference state in which molecules exist as monomers forming an ideal gas mixture. Once the reversible work is obtained as a function of monomer concentration of acid molecules, it is an easy task, if so desired, to re-express it as a function of the number density of all sulfuric acid molecules calculated regardless of hydration state.[14,18,22] The same applies to the total number of water molecules if hydrate formation leads to a serious depletion of water.[22,92]

Inside the vapor phase, we take a system of volume V which satisfies the following two conditions.[93] On one hand, V is sufficiently macroscopic in the sense that its coupling with the surrounding vapor is sufficiently weak. Then the statistical properties of the system are determined by the grand canonical ensemble.[94] On the other hand, V is small enough that the probability of finding more than one uncor-

TABLE VII. Energy and geometry of $HSO_4^- \cdot H_3O^+$ ionic complex. Comparison between simulation and ab initio results.

	This work[a]	''Exact'' value[b]
Energy [kcal/mol]	−136.39	−136.39
O-O_1 distance [Å][c]	2.380	2.326
$\angle O_1$-H_1-O[c]	174.6°	180°
$\angle O_1$-H-O[c]	168.9°	180°

[a]Simulation was carried out at 0.1 K.
[b]Ab initio SCF-MO-LCGO calculation by Kurdi and Kochanski (Ref. 67).
[c]H and O are the atomic sites on hydronium ion, O_1 is on sulfuric acid, and H_1 refers to the position of the proton if the S-O_1 bond is shortened to 1.48 Å without removing H_1 from H_2SO_4.

related density fluctuation that participates in the nucleation process at any instant is negligible, which implies that there is at most one cluster in the system. Then, the reversible work W^{rev} to form a cluster inside V from the reference state is given by

$$\beta W^{rev} = -\log \frac{\Xi^c}{\Xi^r}, \qquad (2)$$

where $\beta \equiv (k_B T)^{-1}$ with k_B and T being the Boltzmann constant and the absolute temperature, respectively. Ξ^r is the partition function of the system constrained to be in the reference state, while Ξ^c is evaluated under the constraint that the system contains a cluster. Assuming the ideal gas behavior in the reference state,

$$\Xi^r(T,V,\mu_w,\mu_s) = \sum_{N_w=0}^{\infty} \sum_{N_a=0}^{\infty} \frac{1}{N_w!} \left(\frac{q_w e^{\beta \mu_w}}{\Lambda_w^3} V\Omega \right)^{N_w}$$
$$\times \frac{1}{N_a!} \left(\frac{q_s e^{\beta \mu_s}}{\Lambda_s^3} V\Omega \right)^{N_a} = e^{(n_w+n_s)V}, \qquad (3)$$

where the subscripts w and s refer to water and sulfuric acid, respectively. The molecular partition functions of the α molecule are given by q_α and Λ_α^3, the former arising from the internal degrees of freedom of the molecule and the latter from the kinetic energy of translation and rotation. μ_α is the chemical potential of the α component in the reference state and Ω arises from the integration over the orientational coordinates of a molecule. Here, the symmetry number of a molecule is absorbed in q_α. Finally, n_α is the number density of the α component in the reference state, where we have made use of the fact that

$$n_\alpha = \frac{q_\alpha e^{\beta \mu_\alpha} \Omega}{\Lambda_\alpha^3}. \qquad (4)$$

In a single component system, a cluster simulation is commonly realized by confining a fixed number of molecules, say i, in a spherical container of volume v concentric with the center of mass of i molecules. To the extent that these molecules actually form a cluster and the thermodynamic properties of the cluster are nearly independent of v over a wide range of v, Lee et al.[34] characterized the cluster by its size i alone. The exclusive use of a canonical ensemble in cluster simulation stems from the fact that clusters are

unstable with respect to change in their size. In the H_2SO_4/H_2O binary system, there are as many as 300 clusters assuming that the maximum numbers of H_2SO_4 and H_2O molecules in a cluster are 3 and 100, respectively. If a canonical ensemble is employed, expensive thermodynamic integration has to be carried out to evaluate the free energy of each cluster. One can significantly reduce the computational effort by devising a simulation that preferentially samples clusters relevant in nucleation, i.e. those found along the valley passing through the saddle point of the reversible work surface. Under conditions typical of sulfuric acid-water binary nucleation, $n_s \ll n_w$. Moreover, when the relative humidity is less than 100%, the sulfuric acid hydrate cannot grow indefinitely without acquiring more acid molecules. Thus, during the time period required for a cluster to either acquire or lose an acid molecule, the cluster reaches *stable* partial equilibrium with respect to its internal degrees of freedom and the exchange of water molecules.[12,14,15] These clusters in *stable* partial equilibrium are, in fact, those found along the valley of the free energy surface. Thus if we employ the mixed ensemble in which the number of water molecules is allowed to fluctuate while that of sulfuric acid molecules is fixed, simulation will preferentially generate the clusters relevant in nucleation. In this approach, a cluster is characterized only by the number N_a^c of sulfuric acid molecules in it. For brevity, we refer to this cluster as the N_a^c cluster. Our goal here is to express Ξ^c in terms of the partition function of the N_a^c cluster in the mixed ensemble. As we shall discuss in Sec. IV, the free energy of the cluster characterized by both N_a^c and N_w^c, the latter being the number of water molecules in it, can be easily obtained from simulation on the N_a^c cluster.

Recently, we developed a new approach to cluster simulation in a single component system using a grand canonical ensemble.[95] The method is free of any arbitrariness involved in the definition of a cluster. Instead, it preferentially generates the physical clusters, defined as the density fluctuations that participate in nucleation,[35–40] and directly determines their equilibrium distribution without the computationally demanding free energy evaluation. In the present case of H_2SO_4/H_2O binary system, however, Monte Carlo moves to create or annihilate an acid molecule will rarely be accepted since a hydrogen bond network will be seriously disturbed in the process. The present approach of using the mixed ensemble can be regarded as an application of the grand canonical ensemble approach to heterogeneous nucleation, in which a fixed number of acid molecules in the cluster, as a whole, are regarded as a heterogeneous nucleation site.

We first obtain the partition function Φ^c for the mixed ensemble under the constraint that the system contains an N_a^c cluster. Once Φ^c is obtained, Ξ^c follows immediately. Since n_s is many orders of magnitude smaller than the corresponding value in the cluster, we can divide the acid molecules in the system to N_a^c belonging to the cluster and N_a^v regarded as part of the vapor. Although no dissociation is allowed in the vapor in accord with the choice of the reference state, possible dissociation in the cluster is an essential feature of the system. We denote the number of resulting bisulfate ions and hydronium ions by N_i. In our model representation of

H_2SO_4/H_2O binary system using the four distinct molecular species, we then have

$$\Phi^c(\beta,V,\mu_w,N_a^v,N_a^c) = \frac{1}{N_a^v!} \left(\frac{q_s V \Omega}{\Lambda_s^3} \right)^{N_a^v} \sum_{N_i=0}^{N_a^c} \frac{1}{(N_a^c - N_i)!}$$

$$\times \left(\frac{q_s}{\Lambda_s^3} \right)^{N_a^c - N_i} \frac{1}{N_i!} \left(\frac{q_b}{\Lambda_b^3} \right)^{N_i} \frac{z_h^{N_i}}{N_i!}$$

$$\times \sum_{N_w=0}^{\infty} \frac{z_w^{N_w}}{N_w!} \int d\{N\} e^{-\beta U_N}, \qquad (5)$$

where the subscripts b and h refer to bisulfate ion and hydronium ion, respectively. We have defined the fugacities z_w of water and z_h of the hydronium ion by

$$z_w \equiv \frac{q_w e^{\beta\mu_w}}{\Lambda_w^3} \quad \text{and} \quad z_h \equiv \frac{q_h e^{\beta\mu_w}}{\Lambda_h^3}, \qquad (6)$$

respectively and assumed that the N_a^v sulfuric acid vapor molecules can be treated as an ideal gas to integrate out their contribution in the configurational integral. As a result, N stands for $N_a^c + N_i + N_w$, whose translational and orientational degrees of freedom are collectively denoted by $\{N\}$ in the configurational integral. Note that in the definition of z_h, Eq. (6), the chemical potential of water is used since hydronium ions are formed from water, to which the system is open. To clarify this point, Eq. (5) is derived in Appendix A starting from a dissociative model. Note that the configurational integral is taken over all configurations consistent with the N_a^c cluster. This constraint is well-defined and presents no difficulty in evaluating the integral. In fact, as we will see below, the partition function to be evaluated by simulation involves only N_a^c acid molecules. Moreover, the boiling point of pure sulfuric acid is much higher ($330\,°C$) than the temperature of interest, where acid molecules are bound together regardless of the value of V. This means that no explicit consideration is necessary to impose the constraint that the N_a^c acid molecules form a cluster. Finally, multiplying Φ^c by $e^{\beta\mu_s(N_a^v + N_a^c)}$ and summing over N_a^v, we can convert Φ^c to Ξ^c:

$$\Xi^c(\beta,V,\mu_w,\mu_s;N_a^c)$$

$$= \sum_{N_a^v=0}^{\infty} e^{\beta\mu_s(N_a^v + N_a^c)} \Phi^c(\beta,V,\mu_w,N_a^v,N_a^c)$$

$$= e^{n_s V} \left(\frac{q_s e^{\beta\mu_s}}{\Lambda_s^3} \right)^{N_a^c} \sum_{N_i=0}^{N_a^c} \frac{\chi^{N_i}}{(N_a^c - N_i)! N_i!} \frac{z_w^{N_i}}{N_i!}$$

$$\times \sum_{N_w=0}^{\infty} \frac{z_w^{N_w}}{N_w!} \int d\{N\} e^{-\beta U_N}, \qquad (7)$$

where χ is defined by

$$\chi = \frac{q_b q_h}{q_s q_w} \frac{\Lambda_s^3 \Lambda_w^3}{\Lambda_b^3 \Lambda_h^3}. \qquad (8)$$

Clearly, $-k_B T \log \chi$ is the free energy of the reaction

$$H_2SO_4 + H_2O \rightarrow HSO_4^- + H_3O^+, \tag{9}$$
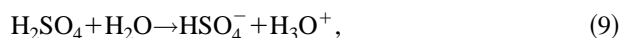
where each molecule is considered to be isolated in vacuum.

If the summation with respect to N_i in Eq. (7) is to be evaluated directly in a single simulation, it must be possible to replace a sulfuric acid-water neutral pair with a bisulfate-hydronium ion pair via a trial move in Monte Carlo simulation. This trial move, however, will almost certainly be rejected since it will seriously disturb the hydrogen bond network in the cluster, costing a very high energy. Instead, each term in the summation over N_i must be calculated separately. In particular, the simulation focuses on evaluating the expression

$$\Xi_w^c(\beta, V, \mu_w, N_a^c, N_i) \equiv \sum_{N_w=0}^{\infty} \frac{z_w^{N_w}}{N_w!} \int d\{N\} e^{-\beta U_N} \tag{10}$$

for each value of N_i, the number of the ion pairs in the system. Except for the analytically tractable factors, Ξ_w^c is the partition function in the mixed ensemble of an N_a^c cluster whose dissociation state is specified by N_i. Equation (10) cannot be evaluated in a single simulation. Instead, it must be evaluated by means of a thermodynamic integration.[33] An expression for $\Xi_w^c(\beta, V, \mu_w, N_a^c, N_i)$ convenient for this purpose is derived in Appendix B. Using Eq. (B6) in Eq. (7), we obtain

$$\Xi^c(\beta, V, \mu_w, \mu_s; N_a^c)$$

$$= e^{(n_s + n_w)V}(n_s V)^{N_a^c} \sum_{N_i=0}^{N_a^c} \frac{n_w^{N_i}}{N_i!(N_a^c - N_i)!}$$

$$\times \left[\frac{\chi}{\Omega} \int d1 \, e^{-\beta u_{hb}(1)} \right]^{N_i} \exp\left\{ -\int_{\beta_0}^{\beta} [\langle U_N \rangle_{n_{w0}} \right.$$

$$\left. -N_i \langle u_{hb} \rangle] d\beta + \int_{\log n_{w0}}^{\log n_w} [\langle N_w \rangle_\beta - n_w V] d \log n_w \right\}, \tag{11}$$

which, when substituted into Eq. (2) along with Eq. (3), yields

$$e^{-\beta W^{rev}(\beta, V, \mu_w, \mu_s; N_a^c)} = (n_s V)^{N_a^c} \sum_{N_i=0}^{N_a^c} e^{-\beta \phi(\beta, V, \mu_w, N_a^c, N_i)}, \tag{12}$$

where we define

$$\beta \phi(\beta, V, \mu_w, N_a^c, N_i)$$

$$\equiv -\log \frac{n_w^{N_i}}{N_i!(N_a^c - N_i)!} + \beta N_i f_{hb}(\beta) + \int_{\beta_0}^{\beta} [\langle U_N \rangle_{n_{w0}}$$

$$-N_i \langle u_{hb} \rangle] d\beta - \int_{\log n_{w0}}^{\log n_w} [\langle N_w \rangle_\beta - n_w V] d \log n_w, \tag{13}$$

where β_0 is chosen to be sufficiently small that the system can be regarded as an ideal gas composed of water, sulfuric acid, and bisulfate-hydronium ion pairs. n_{w0} is the smallest of the number density of water molecules in vapor that we

are interested in and u_{hb} is the intermolecular potential between HSO_4^- and H_3O^+. The thermal average $\langle \cdots \rangle_x$ is evaluated at a fixed value of x, which remains constant along the integration path. The thermal average $\langle u_{hb} \rangle$ is calculated in the canonical ensemble of a single $HSO_4^- \cdot H_3O^+$ ion pair. $f_{hb}(\beta)$ is the free energy required to make the ion pair in the system from sulfuric acid and water forming an ideal gas confined in the unit volume at β and is defined through the relation

$$e^{-\beta f_{hb}(\beta)} \equiv \frac{\chi}{\Omega} \int d1 e^{-\beta u_{hb}(1)}. \tag{14}$$

When n_w is expressed in Å^{-3}, the distance in the integral of Eq. (14) has to be measured in Å so that Eq. (13) is dimensionally consistent.

IV. REVERSIBLE WORK SURFACE AND THE CLUSTER SIZE DISTRIBUTION

In the previous section, a cluster is characterized by N_a^c alone. In the classical nucleation theory, however, it is customary to characterize a cluster by both N_a^c and N_w^c. To obtain the expression for the reversible work to form this (N_a^c, N_w^c) cluster, we must first specify how to define N_w^c for a particular configuration of molecules in the system. Let us consider an excess quantity defined by

$$N_w^{ex} \equiv N_w - n_w V, \tag{15}$$

which is zero for a uniform vapor. However, during a simulation in the mixed ensemble, N_w, and hence N_w^{ex}, fluctuates. For a macroscopic V, this fluctuation arises primarily from that due to the vapor molecules. Fluctuations of this kind have very little to do with the nucleation process and should not be counted as part of a cluster. In the mixed ensemble, however, their effect on N_w^{ex} can be made negligible by decreasing the volume until it satisfies

$$n_w V \ll 1. \tag{16}$$

In this limit, the system contains, on average, no vapor molecule. In fact, the probability of finding at least one vapor molecule of water in the system is, assuming the ideal gas behavior of the vapor phase, given by $1 - e^{-n_w V} \approx n_w V$, which is negligible as a result of Eq. (16). Thus, one can attribute the non-zero value of N_w^{ex} to the presence of a cluster, which suggests that one may define

$$N_w^c \equiv N_w^{ex} + N_i = N_w + N_i - n_w V, \tag{17}$$

where we include hydronium ions in the definition since the ions are formed from water. In view of Eq. (16), we may redefine N_w^c by

$$N_w^c \equiv N_w + N_i, \tag{18}$$

namely, all the water molecules, whether or not protonated, in the system can be regarded as a part of the cluster. The (N_a^c, N_w^c) cluster thus defined is a physical cluster in the sense that it represents density fluctuations relevant in nucleation.[95]

We note that the clusters generated in simulation are consistent with an intuitive definition of clusters. To see this,

note that, except when $N_w^c = 0$, N_w^c is always larger than $n_w V (\ll 1)$, the average number of water molecules in V when filled with the uniform vapor. Thus, on average, any attempted Monte Carlo move to create a molecule in the system will be accepted with higher probability if the newly created molecule interacts more favorably with the rest of the molecules, while as soon as a molecule evaporates from the cluster, it is more likely to be removed from the system upon its trial annihilation.

Some comments on V are in order. Clearly, V has to be larger than the spatial extent of a cluster in it. That the system is microscopic does not affect the applicability of the statistical mechanical description. It is sufficient to assume a weak coupling between the system and its surroundings.[94] Both conditions are trivially satisfied in the present case of vapor to liquid nucleation, where the molar volume in the vapor phase is considerably larger than a physical dimension of the cluster and the interaction between the vapor molecules and a cluster can be ignored.

The expression for the reversible work to form an (N_a^c, N_w^c) cluster can be easily obtained. In fact, the grand canonical partition function Ξ^c of the (N_a^c, N_w^c) cluster is obtained from Eq. (7) by keeping only the term $N_w = N_w^c - N_i$ in the sum over N_w. Thus,

$$\Xi^c(\beta, V, \mu_w, \mu_s ; N_a^c, N_w^c)$$

$$= e^{n_s V} \left(\frac{q_s e^{\beta \mu_s}}{\Lambda_s^3} \right)^{N_a^c} \sum_{N_i=0}^{N_a^c} \frac{\chi^{N_i}}{(N_a^c - N_i)! N_i!} \frac{z_w^{N_i}}{N_i!} \frac{z_w^{N_w}}{N_w!}$$

$$\times \int d\{N\} e^{-\beta U_N}$$

$$= e^{n_s V} \left(\frac{q_s e^{\beta \mu_s}}{\Lambda_s^3} \right)^{N_a^c} \sum_{N_i=0}^{N_a^c} \frac{\chi^{N_i}}{(N_a^c - N_i)! N_i!} \frac{z_w^{N_i}}{N_i!}$$

$$\times \Xi_w^c(\beta, V, \mu_w, N_a^c, N_i) p(\beta, V, \mu_w, N_a^c, N_i, N_w^c - N_i), \tag{19}$$

where p is defined by

$$p(\beta, V, \mu_w, N_a^c, N_i, N_w) \equiv \frac{\dfrac{z_w^{N_w}}{N_w!} \int d\{N\} e^{-\beta U_N}}{\displaystyle\sum_{N_w=0}^{\infty} \frac{z_w^{N_w}}{N_w!} \int d\{N\} e^{-\beta U_N}}, \tag{20}$$

which is the normalized probability of finding N_w water molecules in the system containing N_a^c acid molecules, N_i of which are ions, and is directly obtained from a single simulation. Since Eq. (19) differs from Eq. (7) only by a factor of p, one can obtain the desired expression from Eq. (12):

$$e^{-\beta W^{rev}(\beta, V, \mu_w, \mu_s ; N_a^c, N_w^c)}$$

$$= (n_s V)^{N_a^c} \sum_{N_i=0}^{N_a^c} e^{-\beta \phi(\beta, V, \mu_w, N_a^c, N_i)}$$

$$\times p(\beta, V, \mu_w, N_a^c, N_i, N_w^c - N_i). \tag{21}$$

The equilibrium cluster size distribution $c(\beta, \mu_w, \mu_s, N_a^c, N_w^c)$ can be obtained as follows. Suppose

that the entire vapor phase of volume V_{tot} is divided into small cells of volume V. Because of Eq. (16) and $n_s \ll n_w$, most of the cells contain no molecules at all and those containing a cluster or a monomer are on average spatially distant. Thus, one can assume that all of the cells are statistically independent. Then, the average total number of the (N_a^c, N_w^c) clusters in V_{tot} is given by

$$\frac{V_{tot} \, \Xi^c(\beta, V, \mu_w, \mu_s ; N_a^c, N_w^c)}{V \, \Xi(\beta, V, \mu_w, \mu_s)}, \tag{22}$$

where Ξ is the grand canonical partition function of the system of volume V taken in the vapor. In calculating Ξ, all the possible microstates consistent with the metastable state have to be accounted for. However, since the system contains no molecules at all for most of the time, it can be approximated as ideal gas:

$$\Xi(\beta, V, \mu_w, \mu_s) \approx \Xi^r(\beta, V, \mu_w, \mu_s). \tag{23}$$

When divided by V_{tot}, Eq. (22) becomes

$$c(\beta, \mu_w, \mu_s, N_a^c, N_w^c) = \frac{e^{-\beta W^{rev}(\beta, V, \mu_w, \mu_s ; N_a^c, N_w^c)}}{V}, \tag{24}$$

where we used Eq. (2). As Eq. (2) indicates, $e^{-\beta W^{rev}}$ is the probability of finding the (N_a^c, N_w^c) cluster in the system relative to the reference state. Since the cluster can be found anywhere in the system and the event of finding it at one place or another is mutually exclusive, $e^{-\beta W^{rev}}$ is proportional to V, indicating that c is independent of volume as required.

Finally, we address a consistency issue. Strictly speaking, neither the $(0,1)$ cluster nor the $(1,0)$ cluster is a vapor monomer of water or acid molecule, respectively, since these clusters exclude water vapor from the system of volume V because of the definition Eq. (18), while the monomers do not. In fact, one can readily show that

$$c(1,0) = n_s e^{-n_w V}, \tag{25}$$

where the term for $N_i = 1$ is ignored in Eq. (19), and that

$$c(0,1) = n_w e^{-n_w V}. \tag{26}$$

However, this distinction is completely insignificant since $e^{-n_w V} \approx 1$. Alternatively, one can consistently recover the monomer densities by setting $V = 0$ in Eqs. (25) and (26).

V. DETAILS OF THE SIMULATION

First, we briefly describe some of the details of the simulation. The system is defined as a spherical cavity of radius 50 Å. We studied the clusters of $N_a^c = 1,2,3$. As pointed out in Sec. III, for a given value of N_a^c, there are $N_a^c + 1$ clusters to be simulated separately corresponding to the different dissociation states defined by N_i. Thus, there are nine clusters in total. For each of the clusters, the initial configuration of the molecules is created as follows. The sulfur site of a sulfuric acid molecule or a bisulfate ion is placed at the center of the cavity and the rest of the molecules, including a certain number of water molecules, are placed randomly inside the system. After sufficient equilibration at $T = 303.15$ K and $n_w = 0.1048 \times 10^{-6}$ Å^{-3}, corresponding to a relative humidity
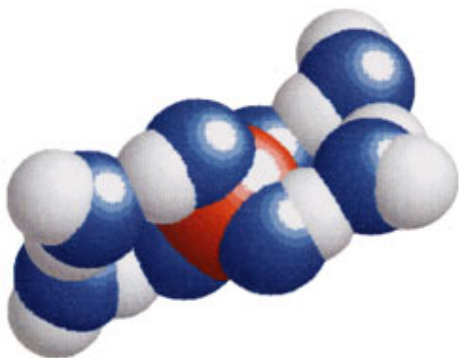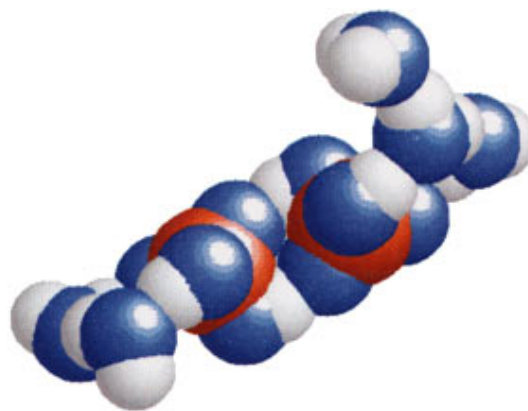
TABLE VIII. Conditions of the simulation. $T = 298.15$ K, and $n_s^{tot} = 0.1 \times 10^{-13}$ Å^{-3}.

No.	n_w [Å^{-3}]	$n_w V$	Relative humidity [%][a]
S1	0.1048×10^{-6}	0.5487×10^{-1}	13.65
S2	0.2×10^{-6}	0.1047	26.06
S3	0.3×10^{-6}	0.1571	39.08
S4	0.3839×10^{-6}	0.2010	50.01
S5	0.5×10^{-6}	0.2618	65.13
S6	0.6×10^{-6}	0.3142	78.17

[a]Saturation pressure of water is assumed to be 23.71 mmHg (Ref. 96).

of about 10% if the actual vapor pressure of water is used,[96] the configuration is used as the initial configuration for the simulations at the nearby values of T and n_w. The process is repeated to obtain the initial configuration of the whole range of T and n_w studied. After equilibration, which typically takes $10^5 – 10^6$ Monte Carlo steps, N_w and U_N are sampled for about $10^7 – 10^9$ Monte Carlo steps. Sampling is made every 10^3 steps for short runs and every 10^4 steps for long runs. Here, one Monte Carlo move consists of (i) trial random translation and rotation of molecules in the system and (ii) one trial grand canonical move, namely a trial creation or annihilation of a water molecule. Molecules to be moved are chosen randomly so that each molecule is picked up once per Monte Carlo step on average. The maximum displacement for a trial translation and the maximum angle for a trial rotation are tuned during the simulation so that the acceptance ratio, defined as the ratio between the number of accepted trial moves and the total number of the trial moves, stays around 50%. As discussed in Appendix C, a molecule at the center of the system undergoes rotation only.

To evaluate the temperature integration in Eq. (13), simulation is performed at 298.15 K and higher temperatures, the highest of which is chosen so that the integrand $[\langle U_N \rangle_{n_{w0}} - N_i \langle u_{hb} \rangle]$ is negligible at this temperature and depends on the values of both N_a^c and N_i. For example, it is 500 K for $(N_a^c, N_i) = (1,0)$, while 2400 K for $(N_a^c, N_i) = (3,3)$. Also, $n_{w0} = 0.1048 \times 10^{-6}$ Å^{-3}. In evaluating the second integral of Eq. (13), simulation is carried out at $n_w = 0.1048 \times 10^{-6}$, 0.2×10^{-6}, 0.3×10^{-6}, 0.3839×10^{-6}, 0.5×10^{-6}, and 0.6×10^{-6} Å^{-3} as summarized in Table VIII.

FIG. 3. A cluster with $N_a^c = 2$, $N_i = 0$ at $T = 298.15$ K and $n_w = 0.5 \times 10^{-6}$ Å^{-3}.

Further technical details of the simulation is discussed in Appendices B–D. In Appendix B, a criterion is discussed on the adequacy of the number of intermediate points used to evaluate the thermodynamic integrations. In Appendix C, a criterion in choosing the system volume V is discussed from a point of view somewhat different from that of Lee *et al.*[34] Finally, under a reasonable approximation, one can dispense with the integration with respect to n_w indicated in Eq. (13), which results in the improvement of the computational efficiency by a factor of several. The method is discussed in Appendix D.

VI. RESULTS AND DISCUSSION

A. Shape of the clusters

Snapshots[97] of the clusters are shown in Figs. 2–7, where sulfur sites, oxygen sites, and hydrogen sites are colored red, dark blue, and white, respectively. Figure 2 shows a hydrate of a sulfuric acid molecule, in which a loop of hydrogen bonds is formed from the H_1 site to the O_2 site of the acid with two water molecules, similarly for $H_{1'}$ to $O_{2'}$. In hydrates with fewer water molecules, the hydrogen bonds are formed preferentially from the H_1 and $H_{1'}$ protons to oxygens of water molecules. One end of the hydrogen from a water attached to the H_1 site, for example, forms a distant hydrogen bond to the O_2 site.
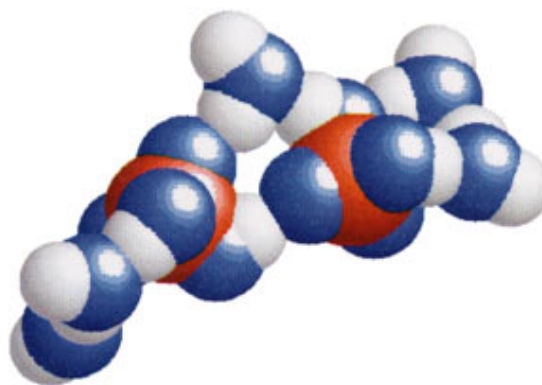

FIG. 2. A cluster with $N_a^c = 1$, $N_i = 0$ at $T = 298.15$ K and $n_w = 0.6 \times 10^{-6}$ Å^{-3}.
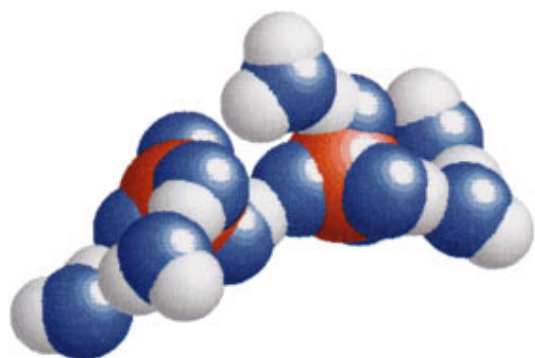

FIG. 4. A cluster with $N_a^c = 2$, $N_i = 0$ at $T = 298.15$ K and $n_w = 0.6 \times 10^{-6}$ Å^{-3}.

FIG. 5. A cluster with $N_a^c = 2$, $N_i = 0$ at $T = 298.15$ K and $n_w = 0.6 \times 10^{-6}$ Å^{-3}.

FIG. 7. A cluster with $N_a^c = 3$, $N_i = 0$ at $T = 298.15$ K and $n_w = 0.6 \times 10^{-6}$ Å^{-3} showing a ring conformation.

Figures 3, 4, and 5 show clusters with two sulfuric acid molecules. Note that the acid molecules directly form two hydrogen bonds in Fig. 3, while one of them is mediated by a water molecule in Fig. 4. Around room temperature and at all values of n_w investigated in this work, these two configurations are representative of the connectivity of the acid molecules. Since interconversion of these two conformations requires one or two hydrogen bonds to be broken first, the Monte Carlo lifetimes of the conformations are fairly long, being of the order of 10^7 steps. As the value of n_w is increased, configurations similar to Fig. 4 become more probable than those similar to Fig. 3. The configuration in Fig. 5 can be regarded as an intermediate between those two. Note that $N_w^c = 5$ in both Figs. 3 and 4. However, it is unlikely that interconversion between these two conformations occurs in a canonical simulation since it would involve diffusion of a water molecule over several angstroms on the cluster surface where no favorable interaction site exists. This shows a clear advantage of the mixed ensemble simulation over a conventional one in a canonical ensemble. This effectiveness in sampling very different relevant configurations has been stressed in a simulation work that determines the solvation shell structure of protein and nucleic acid,[98] for example.

Similar connectivity is observed in Fig. 6 for clusters with three sulfuric acid molecules. An additional complication arises in this case, however, since the acid molecules can now form a ring (Fig. 7). As is seen from Figs. 6 and 7, acid
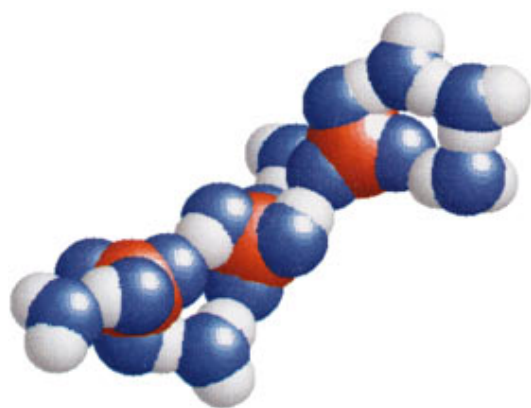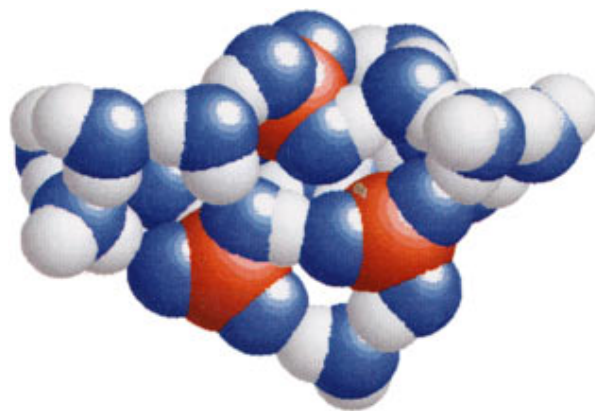
molecules in the ring conformation tend to form hydrogen bonds preferentially with water molecules than among themselves in comparison to those in the linear conformation, leading to larger clusters. Since both conformations are observed in the simulation, the corresponding free energies are expected to be close, the difference being the order of $k_B T$. To understand its implication, we monitored the quantity

$$\beta W \equiv \beta U_N - \log \frac{(n_w V)^{N_w}}{N_w!}, \qquad (27)$$

which plays the same role as βU_N in a canonical ensemble in that the statistical weight of a given microstate is proportional to $e^{-\beta W}$. The data from simulation of 7×10^8 Monte Carlo steps were divided into small blocks, each of which corresponding to 10^7 Monte Carlo steps, and the average of βW was calculated for each block. Figure 8 shows the variation of this block average of βW for three values of n_w. Larger, i.e., less negative, values of βW correspond to the linear conformation while the smaller values of βW correspond to the ring conformation. Despite the large difference in βW, both linear and ring conformations are observed. This means that the ring conformation is entropically unfavorable since it attracts more water molecules, confining them to a far smaller volume than V. As these water mol-
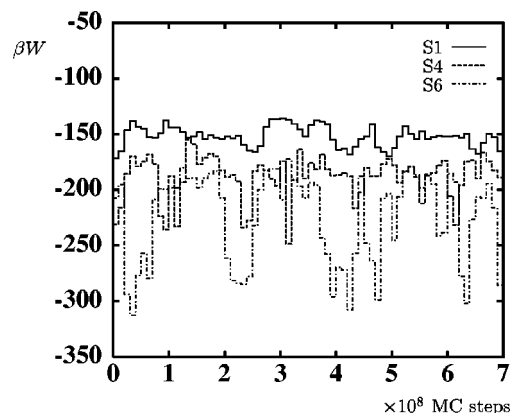

FIG. 6. A cluster with $N_a^c = 3$, $N_i = 0$ at $T = 298.15$ K and $n_w = 0.6 \times 10^{-6}$ Å^{-3} showing a linear conformation.

FIG. 8. The change in the block average of βW. The size of each block is 10^7 MC steps. The conditions of simulation for S1, S4, and S6 are given in Table VIII.

TABLE IX. Heat of formation.

Molecule	ΔH_f [kcal/mol]
H_2O[a]	-57.80
H_2SO_4[b]	-175.67 ± 1.912
H_3O^{+}[a]	142 ± 1
HSO_4^{-}[b]	-227.77 ± 4.063

[a]Prigogine and Defay (Ref. 105).
[b]Lias et al. (Ref. 106).

ecules evaporate, the cluster returns to the linear conformation. From Fig. 8, it is clear that additional Monte Carlo steps are required to achieve good statistics. Nonetheless, qualitative trends are already present. For example, the ring conformation appears more frequently as n_w is increased.

None of the clusters shown here possesses a spherical or an axial symmetry. Given the fairly long lifetime of each conformation of the clusters, the same is expected to be true even after the thermal average is taken. Thus, the thermodynamic description of the clusters is no longer amenable to Gibbs' prescription.[57] In particular, the thermodynamic quantities cannot be classified into extensive and intensive ones, which is a prerequisite in deriving the familiar Gibbs–Duhem relation, for example. It seems hardly profitable to try to extend Gibbs' interfacial thermodynamics to include such cases, since the quantities introduced into such a theory are unlikely to be subject to experimental measurement. This in turn highlights the importance of the molecular level approach.

B. Estimate of the value of f_{hb}

To evaluate the reversible work to form an N_a^c cluster or an (N_a^c, N_w^c) cluster, from Eqs. (12) or (21), the value of f_{hb} defined by Eq. (14) is required. Using the heat of formation of the molecules given in Table IX and ignoring the entropic effect, we obtain

$$-k_B T \log \chi \approx 147.70 \pm 6.98 \quad \text{kcal/mol.} \quad (28)$$

To evaluate the remaining factor in Eq. (14), we introduce the approximation

$$\frac{1}{\Omega} \int d1 \, e^{-\beta u_{hb}(1)} \approx \frac{v_f \omega_f}{\Omega} e^{-\beta \langle u_{hb} \rangle}, \quad (29)$$

where v_f and ω_f respectively denote the volume and the solid angle over which H_3O^{+} can fluctuate with respect to HSO_4^{-}. We approximate their values as the cubic of the maximum displacement and angle used for the trial Monte Carlo move. Then

$$v_f \approx 0.25^3 \quad \text{Å}^3, \quad \omega_f \approx 0.3^3. \quad (30)$$

From simulation, $\langle u_{hb} \rangle = 135.04 \pm 0.01$ kcal/mol at $T = 298.15$ K. Since Å^3 in v_f cancels out Å^{-3} of n_w in Eq. (13), we can omit the unit of volume here to obtain

$$-k_B T \log \frac{1}{\Omega} \int d1 \, e^{-\beta u_{hb}(1)} \approx -127.85 \pm 0.01 \quad \text{kcal/mol.} \quad (31)$$
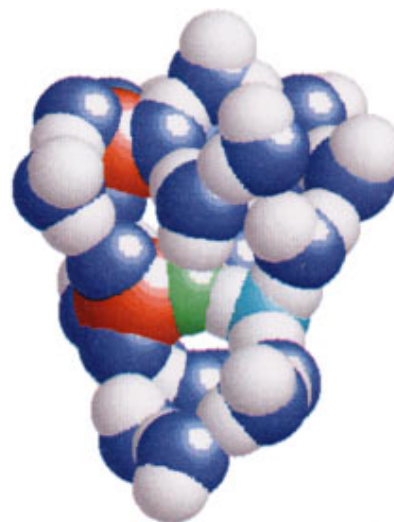
Combining Eqs. (28) and (31), we obtain

FIG. 9. A cluster with $N_a^c = 2$, $N_i = 1$ at $T = 298.15$ K and $n_w = 0.6 \times 10^{-6}$ Å^{-3}.

$$f_{hb} \approx 19.85 \pm 6.99 \quad \text{kcal/mol.} \quad (32)$$

In what follows, we adopt 20 kcal/mol as the value of f_{hb}. At $T = 298.15$ K, the indicated uncertainty in this quantity is as large as $12 k_B T$. Effects of this uncertainty will be addressed subsequently.

C. Dissociation of H_2SO_4 in a cluster

Snapshots of clusters containing a $HSO_4^{-} \cdot H_3O^{+}$ ion pair are shown in Figs. 9 and 10, in which atomic sites are colored as before with the exceptions for the O_1 site of the bisulfate ion and the oxygen site of the hydronium ion, which are, respectively, colored green and light blue. In Fig. 9, a hydrogen from H_3O^{+} forms a hydrogen bond directly to the O_1 site of HSO_4^{-}, while in Fig. 10, H_3O^{+} forms hydrogen bonds to oxygen sites of H_2O and H_2SO_4. In both clusters, however, there is no intervening molecule between the ion pair. The same holds true for ion pairs buried in 97 water molecules as shown in Fig. 11. The water molecules start to intervene in the ion pairs as the number of water molecules exceeds about 240 as shown in Fig. 12. Thus our simulation
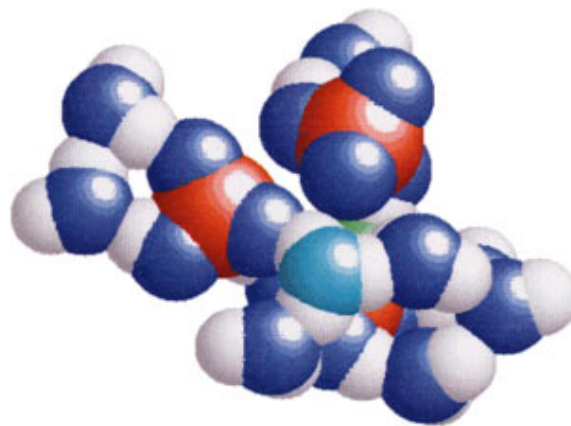

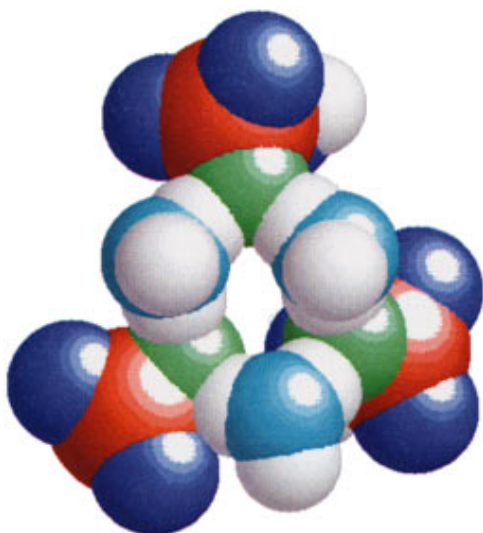FIG. 10. A cluster with $N_a^c = 3$, $N_i = 1$ at $T = 298.15$ K and $n_w = 0.3839 \times 10^{-6}$ Å^{-3}.

FIG. 11. Ion pairs forming a core inside the cluster with $N_w^c = 97$. $N_a^c = 3$, $N_i = 3$ at $T = 298.15$ K and $n_w = 0.6 \times 10^{-6}$ Å^{-3}. Water molecules are not shown.

FIG. 13. Free energy of the N_a^c cluster as a function of the dissociation state defined by N_i. $N_a^c = 3$ and $T = 298.15$ K. $f_{hb} = 20$ kcal/mol. The conditions of simulation for S1, S3, and S5 are given in Table VIII.

suggests that, as far as the dissociation behavior of H$_2$SO$_4$ is concerned, at least about 240 water molecules are required to attain a behavior that resembles the bulk solution.

The fact that there is no separation of ion pairs in a small cluster does not imply that dissociation is not important in the cluster. As an H$_2$SO$_4 \cdot$H$_2$O neutral dimer dissociates to an HSO$_4^- \cdot$H$_3$O$^+$ ion pair, its net dipole moment increases to attract more water molecules. (If these dimers are placed in vacuum, the dipole moment changes from 3.28 D to 12.0 D at 298.15 K upon dissociation.) Consequently, the potential energy of the cluster decreases. Whether or not dissociation occurs in a given N_a^c cluster is determined by the free energy $\phi(N_a^c, N_i)$, defined by Eq. (13), of the cluster as a function of N_i. The quantity is shown in Fig. 13 for the case of $N_a^c = 3$ at $T = 298.15$ K for three values of n_w. Clearly, dissociation occurs for all cases. The increase in $\beta\phi$ is observed as N_i changes from 0 to 1 when $n_w = 0.1048 \times 10^{-6}$ Å^{-3}, reflecting the fact that the ion pair cannot attract sufficient water molecules when placed in vapor with such a low water
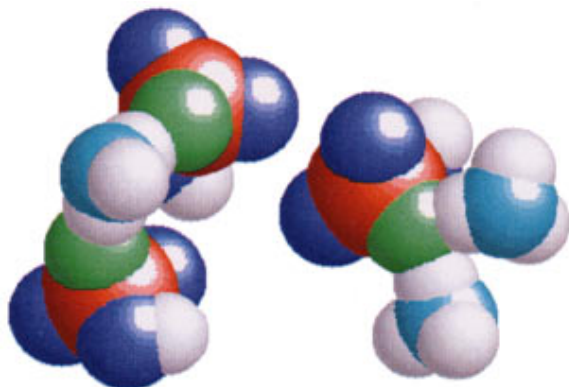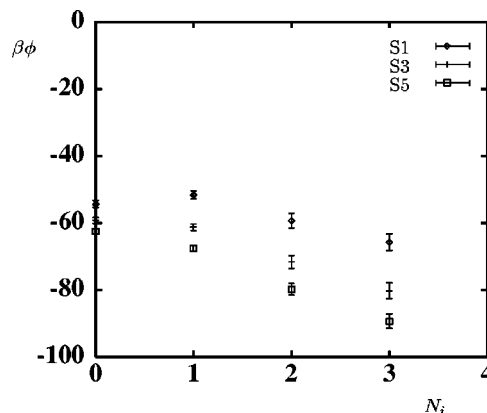
concentration. If 27 kcal/mol is assumed for the value of f_{hb}, however, we find that dissociation no longer occurs for this N_a^c cluster (Fig. 14). This change at the qualitative level points to the necessity of a more accurate estimate of the value f_{hb}.

D. Effect of hydration

In Eqs. (12) and (21), n_s represents the number density of unhydrated sulfuric acid molecules in accordance with the choice of our reference state in calculating the reversible work. In reality, however, most acid molecules exist as hydrates and one can specify only the total number density n_s^{tot}. Thus, we must express n_s in terms of n_s^{tot}. The derivation given here is analogous to the corresponding one in the classical theory.[14,18,22]

Since a given acid molecule is either hydrated or unhydrated regardless of its dissociation state, we have

$$n_s^{tot} = \sum_{N_a^c = 1} \sum_{N_w^c} N_a^c \, c(N_a^c, N_w^c). \qquad (33)$$
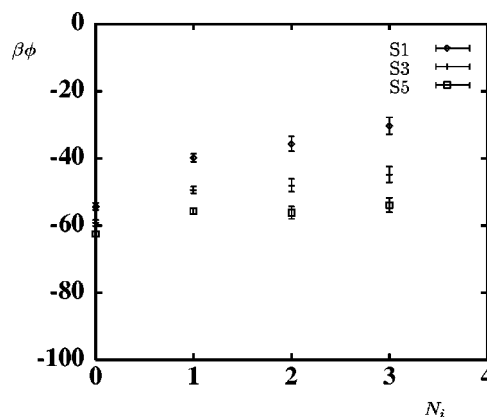
From Eqs. (21) and (24), we obtain

FIG. 12. Ion pairs forming a core inside the cluster with $N_w^c = 243$. $N_a^c = 3$, $N_i = 3$ at $T = 298.15$ K and $n_w = 0.6 \times 10^{-6}$ Å^{-3}. Water molecules are not shown.

FIG. 14. Free energy of the N_a^c cluster as a function of the dissociation state defined by N_i. $N_a^c = 3$ and $T = 298.15$ K. $f_{hb} = 27$ kcal/mol. The conditions of simulation for S1, S3, and S5 are given in Table VIII.

$$n_s^{tot} = \frac{1}{V} \sum_{N_a^c=1} N_a^c \, (n_s V)^{N_a^c} \sum_{N_i=0}^{N_a^c} e^{-\beta\phi(N_a^c, N_i)}, \qquad (34)$$

where we have made use of the normalization condition

$$\sum_{N_w=0} p(\beta, V, \mu_w, N_a^c, N_i, N_w) = 1. \qquad (35)$$

Assuming that the hydrates are dominated by those containing only one acid molecule ($N_a^c = 1$), we find that

$$p_0 \equiv \frac{n_s}{n_s^{tot}} \approx \left[\sum_{N_i=0}^{1} e^{-\beta\phi(1,N_i)} \right]^{-1}. \qquad (36)$$

In the following, we assume that $n_s^{tot} = 0.1 \times 10^{-13}$ Å^{-3}, which is typical of experiments in H$_2$SO$_4$/H$_2$O binary nucleation.[32]

E. Reversible work of cluster formation and comparison with the classical predictions

Recall that the cluster size distribution is given in the classical nucleation theory by

$$c(N_a^c, N_w^c) = n_w \exp[-\beta W^{classical}(N_a^c, N_w^c)], \qquad (37)$$

where $W^{classical}$ is the reversible work of cluster formation evaluated by the classical theory. Thus, rewriting Eq. (24) as

$$c(N_a^c, N_w^c) = n_w \exp[-\beta W^{rev}(N_a^c, N_w^c) - \log(n_w V)], \qquad (38)$$

we find that a sensible comparison is made between our molecular theory and the classical by comparing the quantity defined by

$$\beta w^{REV(N_a^c, N_w^c)} \equiv \beta W^{rev}(N_a^c, N_w^c) + \log(n_w V) \qquad (39)$$

against $\beta W^{classical}(N_a^c, N_w^c)$. Similar quantities can be defined for an N_a^c cluster by summation with respect to N_w^c of Eqs. (37) and (38). Thus, we compare $W^{classical}(N_a^c)$ defined by

$$\exp[-\beta W^{classical}(N_a^c)]$$
$$\equiv \sum_{N_w^c=0}^{\infty} \exp[-\beta W^{classical}(N_a^c, N_w^c)] \qquad (40)$$

with $w^{REV}(N_a^c)$ defined by

$$\exp[-\beta w^{REV}(N_a^c)] \equiv \sum_{N_w^c=0}^{\infty} \exp[-\beta w^{REV}(N_a^c, N_w^c)]. \qquad (41)$$

The upper limit (∞) of the summation is only formal since the summand decays quickly as N_w^c is increased when the relative humidity is less than 100%.

Figure 15 compares the reversible work βw^{REV} of the N_a^c cluster formation obtained by assuming the value of 20 kcal/mol for f_{hb} with $\beta W^{classical}$ obtained by the classical theory.[99] While the classical theory predicts that a 3-cluster is still subcritical, our simulation predicts that a 2-cluster is the critical nucleus for conditions S1 to S4 and that βw^{REV} decreases monotonically with N_a^c for conditions S5 and S6. (See Table VIII.) This means that the rate-limiting step of
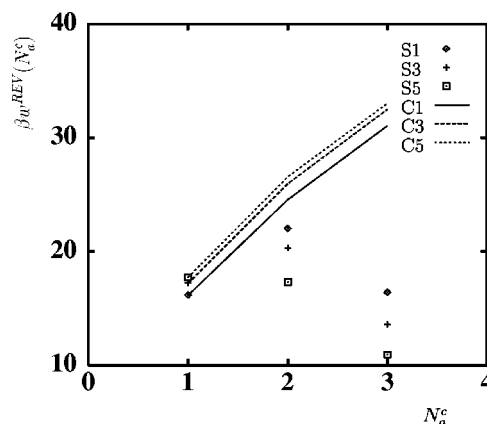

FIG. 15. Reversible work of N_a^c-cluster formation at $T = 298.15$ K. Calculated with $f_{hb} = 20$ kcal/mol. The conditions of simulation for S1, S3, and S5 are given in Table VIII. C1 shows the classical prediction under the condition S1. Similarly for C3 and C5.

new particle formation is the binary collision of sulfuric acid molecules. Note that the classical theory predicts that $\beta W^{classical}$ increases as n_w is increased. This trend reflects the fact that a higher value of n_w results in more significant depletion of the acid molecules and reverses as N_a^c becomes large enough so that the cluster is a critical nucleus. When 27 kcal/mol is employed for the value of f_{hb}, the results of our simulation become more or less comparable with the classical prediction as shown in Fig. 16. This indicates that the large discrepancy between the molecular theory and the classical as observed in Fig. 15 arises from the difference in the behavior of a cluster involving the HSO$_4^-$·H$_3$O$^+$ ion pairs.

To obtain more detailed information regarding the clusters with ion pairs, we calculated βw^{REV} of the (N_a^c, N_w^c)-cluster formation for the condition S3. The results are shown in Figs. 17 and 18 for the case of $f_{hb} = 20$ kcal/mol and 27 kcal/mol, respectively. Figures 17 and 18 also compare the simulation against the classical prediction. For small values of N_w^c the agreement is surprisingly good. Figure 17 shows a double minimum in the reversible work. The
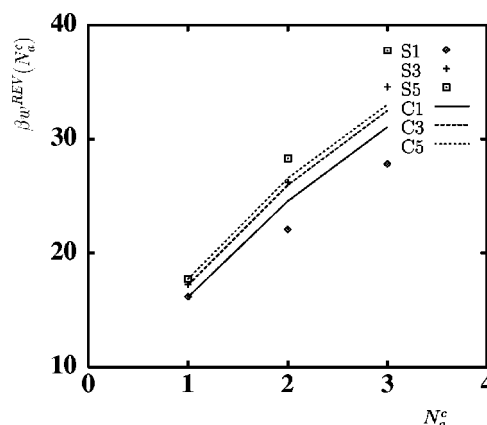

FIG. 16. Reversible work of N_a^c-cluster formation at $T = 298.15$ K. Calculated with $f_{hb} = 27$ kcal/mol. The conditions of simulation for S1, S3, and S5 are given in Table VIII. C1 shows the classical prediction under the condition S1. This is similar for C3 and C5.
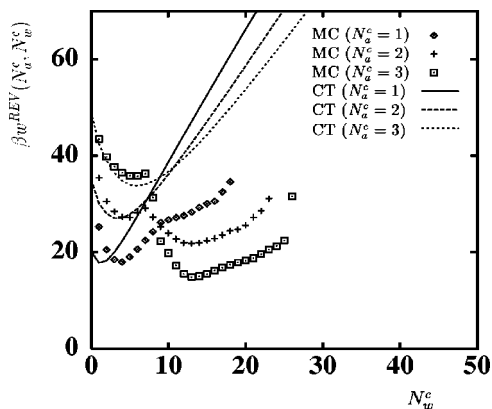
FIG. 17. Reversible work of (N_a^c, N_w^c)-cluster formation at $T = 298.15$ K, $n_w = 0.3 \times 10^{-6}$ Å^{-3}, and $n_s^{tot} = 0.1 \times 10^{-13}$ Å^{-3}. Calculated with $f_{hb} = 20$ kcal/mol. CT and MC denote the classical prediction and the results of simulation, respectively.

minimum for the larger values of N_w^c corresponds to the clusters with ion pairs, while the contribution to the minimum for the smaller values of N_w^c arises from the undissociated states, since the $HSO_4^- \cdot H_3O^+$ ion pair has a larger dipole moment than the $H_2SO_4 \cdot H_2O$ neutral dimer and hence can attract more water molecules (as discussed in Sec. VI C). From Fig. 17, the dominant cluster for the case of $N_a^c = 1$ is the (1,4) cluster. If two (1,4) cluster collide without losing a water molecule, the resulting (2,8) cluster is already in the state with one or two dissociated acid molecules, and hence can attract more water molecule to form a stable cluster. Figure 17 further indicates that, upon acquiring one more sulfuric acid molecule, an even more stable cluster results, implying that binary collision is the rate limiting step. This scenario does not necessarily conflict with the experimental results[31] analyzed using the nucleation theorem,[100–103] which suggest that a critical nucleus contains about 15 acid molecules, since application of the theorem *presumes* that the rate limiting step is nucleation involving a critical nucleus in equilibrium with the surrounding vapor. To appreciate this limitation regarding the validity of the nucleation theorem, recall
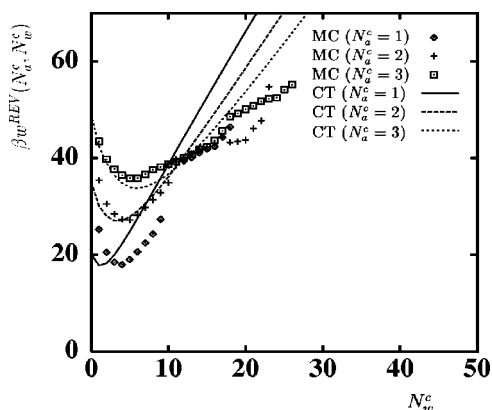

FIG. 18. Reversible work of (N_a^c, N_w^c)-cluster formation at $T = 298.15$ K, $n_w = 0.3 \times 10^{-6}$ Å^{-3}, and $n_s^{tot} = 0.1 \times 10^{-13}$ Å^{-3}. Calculated with $f_{hb} = 27$ kcal/mol. CT and MC denote the classical prediction and the results of simulation, respectively.

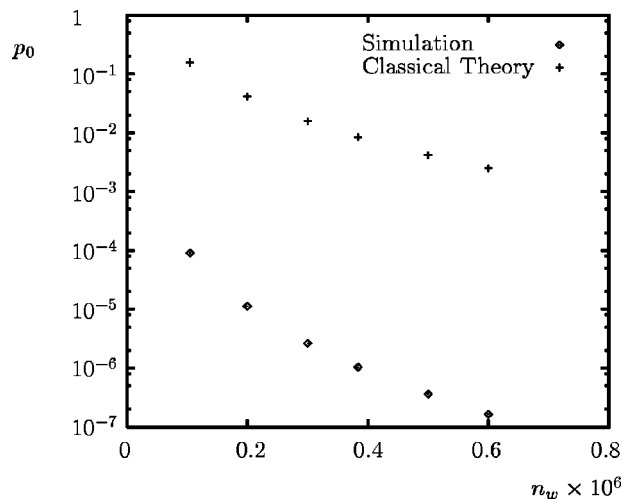FIG. 19. Comparison of the probability that a sulfuric acid molecule is unhydrated. At $T = 298.15$ K and $n_s^{tot} = 0.1 \times 10^{-13}$ Å^{-3}. Calculated with $f_{hb} = 20$ kcal/mol.

that this theorem is a direct consequence of the thermodynamic identity[104]

$$-\langle N_i \rangle \equiv \left(\frac{\partial \psi}{\partial \mu_i} \right)_{T,V,\mu_{j \neq i}}, \qquad (42)$$

where ψ is the grand potential and $\langle N_i \rangle$ is the average number of i-molecules in the system. The identity Eq. (42) holds only at equilibrium where the grand potential is stationary with respect to fluctuation in the density profile. In Fig. 17, we note that the most probable number of water molecules in a 3-cluster is comparable with that in a 2-cluster. This means that some of the water molecules have to evaporate after a 2-cluster captures an acid hydrate. When f_{hb} is increased from 20 kcal/mol to 27 kcal/mol to reflect its uncertainty, the resulting reversible work surface changes markedly and our simulation becomes more or less comparable with the classical prediction. This sensitivity to f_{hb} again stresses the importance of the accurate estimation of this quantity.

Next, we draw attention to the distribution of acid hydrates, for which $N_a^c = 1$. Both Figs. 17 and 18 show that the dominant hydrates contain four water molecules, which is larger than the classical prediction of two hydrating water molecules at relative humidity less than 100%.[14,18,19] To identify the origin of this discrepancy, we calculated the average interaction energy of the $H_2SO_4 \cdot H_2O$ dimer at $T = 298.15$ K and obtained -13.7 kcal/mol, which is 0.9 kcal/mol lower than the classical prediction of the first hydration enthalpy (-12.8 kcal/mol) estimated by Mirabel and Ponche.[13] This difference of 0.9 kcal/mol is far from insignificant. For example, Fig. 19 compares the result of the simulation and the classical predication on the fraction of unhydrated acid molecules p_0 given by Eq. (36). Clearly, our simulation predicts far more significant depletion of the unhydrated acid concentration as a result of hydration. Thus, the agreement between simulation and the classical prediction at small values of N_w^c is most likely a result of the cancellation of errors. Such sensitivity of the hydrates distribution points to the critical importance of an accurate *ab*

initio calculation to enable the accurate determination of the model potentials. We note that p_0 is quite insensitive to the value of f_{hb}, which indicates that no appreciable dissociation occurs in hydrates with one acid molecule as seen also from Figs. 17 and 18. This in turn indicates that the important interaction potential that determines the behavior of p_0 is the H_2SO_4–H_2O interaction. In the present work, we adopted the *ab initio* results of Kurdi and Kochanski.[67] To see the sensitivity of the hydration state of the acid molecule to the molecular parameters, we tested a model of sulfuric acid molecule parametrized using the results by Morokuma and Muguruma[90] given in Table VI. The resulting acid molecule shows no significant hydration. This is a rather unrealistic result and implies that the H_2SO_4—H_2O interaction is stronger than the prediction of Morokuma and Muguruma, adding credibility to our original parametrization.

VII. SUMMARY AND IMPLICATIONS FOR THE CLASSICAL BINARY NUCLEATION THEORY

We have developed a classical mechanical model representation of the H_2SO_4/H_2O binary system. The model has been used in Monte Carlo simulation to obtain a significant section of the free energy surface of binary cluster formation. To our knowledge, this is the first time that such an extensive free energy calculation has been performed for clusters in a binary system. The mixed ensemble simulation is effective both in sampling very different configurations of clusters relevant in homogeneous nucleation and in evaluating the cluster free energy. When the method is used under the approximation discussed in Appendix D, the required computational effort is further reduced, perhaps even to the point less than that required in a canonical ensemble simulation on a single component system involving clusters of comparable size.

Our simulation yields considerable molecular level insight. Clusters observed are highly nonspherical. At conditions typical of H_2SO_4/H_2O binary nucleation, a cluster with a given number of acid molecules has several very different conformations, which are close in free energy and hence equally relevant in nucleation. Each conformation has a fairly long Monte Carlo lifetime. Dissociation behavior of H_2SO_4 in a cluster differs markedly from that in bulk solution and depends sensitively on the assumed value of the free energy f_{hb} of the dissociation reaction $H_2SO_4 + H_2O \rightarrow HSO_4^- \cdot H_3O^+$. In a small cluster, no dissociation is observed. As the cluster size becomes larger, the probability of having an $HSO_4^- \cdot H_3O^+$ ion pair increases. However, in the clusters relevant in nucleation, the resulting ion pairs remain in contact and about 240 water molecules are required to observe the behavior which resembles that in bulk solution. When the assumed value of f_{hb} is increased to reflect its uncertainty, the probability of having the ion pair becomes negligible.

The reversible work obtained from simulation shows quantitative agreement with the classical theory for small clusters, in which dissociation of the acid molecules is unlikely. This is rather surprising since the classical theory assumes the same dissociation behavior in a cluster as in bulk liquid solution. Effect due to the difference in dissociation behavior, in part, will be corrected by the surface term in the classical theory, since dissociation behavior near the bulk vapor-liquid interface also differs from that in bulk solution. Therefore, this agreement just mentioned is attributed, to a large extent, to a cancellation of errors, as discussed in Sec. VI E. For larger clusters, for which dissociation occurs, the status is different. When the $H_2SO_4 \cdot H_2O$ neutral pair dissociates to form the $HSO_4^- \cdot H_3O^+$ ion pair, its dipole moment becomes nearly 4 times larger, thereby stabilizing clusters of large N_w^c, which in turn results in a reversible work surface quite different from the classical prediction, and suggests that the rate-limiting step in stable particle formation is the binary collision of two acid molecules, both of which are likely hydrated. If a value of 27 kcal/mol instead of 20 kcal/mol is assumed for f_{hb}, the reversible work surface appears to be in better accord with the result of the classical theory which predicts a nucleation barrier at experimental conditions typical of H_2SO_4/H_2O nucleation. This apparent agreement, again, is most probably due to a cancellation of errors in the latter since the assumed dissociation behavior of the sulfuric acid molecule in a water cluster in the classical theory is very different from the dissociation behavior observed in our simulation. Because of the uncertainties in the value of f_{hb}, we are unable to conclude which one of the two scenarios, i.e., binary collision vs nucleation, represents what occurs in reality. Therefore, caution must be exercised in applying our model results to real systems. Clearly, further studies are required. On the theoretical side, the sensitivity of our predictions to the parameters used in the model highlights the need for more accurate estimates of these parameters.

APPENDIX A: DERIVATION OF EQ. (5)

Let N_a denote the total number of sulfuric acid molecules in the system of volume V. Although no dissociation is allowed in the vapor in accordance with the choice of the reference state, we take account of the possible dissociation in the cluster. Thus, it is most convenient to start from a classical mechanical partition function of a dissociative model. In view of the fact that the second dissociation of sulfuric acid is negligible compared to the first, we can introduce a model composed of water molecules, bisulfate ions, and protons. The partition function for the system is

$$\Phi^c(\beta,V,\mu_w,N_a;N_a^c)=\frac{1}{N_a!}\left(\frac{q_p}{\Lambda_p^3}\right)^{N_a}\frac{1}{N_a!}\left(\frac{q_b}{\Lambda_b^3}\right)^{N_a}$$

$$\times\sum_{N_w'=0}^{\infty}\frac{1}{N_w'!}\left(\frac{q_we^{\beta\mu_w}}{\Lambda_w^3}\right)^{N_w'}$$

$$\times\int d\{N'\}e^{-\beta U'_{N'}},\qquad(A1)$$

where the total number of bisulfate ions and that of the protons are both denoted by N_a in accordance with the charge neutrality condition, $N'\equiv2N_a+N_w'$ is the total number of molecules, and $U'_{N'}$ is the interaction potential in this dissociative model description, whose explicit form is irrelevant here. The subscripts b and p stand for bisulfate ion and proton, respectively. The translational and orientational degrees freedom of all molecules are collectively denoted by $\{N'\}$ in the configurational integral. As discussed in Sec. II, an accurate representation of $U_{N'}$ is difficult to achieve. Instead, we rewrite Eq. (A1) to reflect the fact that the main contribution to Φ^c comes from the configurations in which protons are chemically bonded to either bisulfate ion or water. Let N_i be the number of protons bonding to water molecules to form hydronium ions. The remaining N_a-N_i protons bond to bisulfate ions to form sulfuric acid molecules. We assume that N_a acid molecules can be divided into N_a^v vapor molecules, for which no dissociation is allowed in accord with the definition of the reference state, and N_a^c molecules belonging to the cluster. The assumption is reasonable since n_s is many orders of magnitude smaller than the corresponding value in the cluster. Then Eq. (A1) can be approximated by

$$\Phi^c(\beta,V,\mu_w,N_a;N_a^c)$$

$$\approx\sum_{N_i=0}^{N_a^c}\sum_{N_w'=N_i}^{\infty}\frac{1}{N_a!}\left(\frac{q_p}{\Lambda_p^3}\right)^{N_a}\frac{1}{N_a!}\left(\frac{q_b}{\Lambda_b^3}\right)^{N_a}$$

$$\times\frac{1}{N_w'!}\left(\frac{q_we^{\beta\mu_w}}{\Lambda_w^3}\right)^{N_w'}N_a!\binom{N_a}{N_a^v}\binom{N_a^c}{N_a^c-N_i}\binom{N_w'}{N_i}$$

$$\times\left[\int d1e^{-\beta u_{pb}(1)}\right]^{N_a-N_i}$$

$$\times\left[\int d1e^{-\beta u_{pw}(1)}\right]^{N_i}\int d\{N\}e^{-\beta U_N},\qquad(A2)$$

where $N\equiv N_a+N_i+N_w$ with N_w denoting the number of water molecules excluding the protonated ones, and U_N is the total intermolecular interaction potential excluding the intramolecular interaction denoted by u_{pb} and u_{pw}. The upper limit of the first summation arises from the fact that dissociation of the sulfuric acid molecules is allowed only for those molecules inside the cluster and hence the number N_i of hydronium ions formed by the accompanying protonation of water cannot exceed N_a^c. The lower limit of the second summation reflects the fact that the hydronium ions thus formed have to remain in the system as a result of the charge neutrality condition. The factor

$$N_a!\binom{N_a}{N_a^v}\binom{N_a^c}{N_a^c-N_i}\binom{N_w'}{N_i}\qquad(A3)$$

is introduced here since the molecules must be regarded as distinguishable in the configurational integral. In Eq. (A3), the factors

$$\binom{N_a}{N_a^v},\quad\binom{N_a^c}{N_a^c-N_i},\quad\text{and}\quad\binom{N_w'}{N_i},$$

respectively denote the number of ways of choosing N_a^v bisulfate ions out of N_a to be protonated and placed in the vapor phase, $N_a^c-N_i$ bisulfate ions to be protonated in the cluster, and N_i water molecules to be protonated in the system. Then, $N_a!$ takes care of all possible permutations of protons among all protonated species. Defining the molecular partition functions by

$$\frac{q_s}{\Lambda_s^3}\equiv\frac{q_pq_b}{\Lambda_p^3\Lambda_b^3}\int d1e^{-\beta u_{pb}(1)}\qquad(A4)$$

and

$$\frac{q_h}{\Lambda_h^3}\equiv\frac{q_pq_w}{\Lambda_p^3\Lambda_w^3}\int d1e^{-\beta u_{pw}(1)},\qquad(A5)$$

we obtain Eq. (5).

APPENDIX B: EVALUATION OF Ξ^c BY A THERMODYNAMIC INTEGRATION

A common procedure[33] to evaluate Eq. (10) relies on the identity

$$\Xi_w^c(\beta,V,\mu_w,N_a^c,N_i)=\Xi_w(\beta_0,V,\mu_w,N_a^c,N_i)$$

$$\times\exp\left[-\int_{\beta_0}^{\beta}\langle U_N\rangle_{z_w}d\beta\right],\quad(B1)$$

where β_0 is chosen to be sufficiently small that the system can be regarded as an ideal gas composed of water, sulfuric acid, and bisulfate-hydronium ion pairs. The subscript x for $\langle\cdots\rangle_x$ reminds us that the quantity x is held constant in evaluating the integration. The procedure implied in Eq. (B1) is not particularly attractive since, if we are to obtain the free energy of a cluster under various values of relative humidity, the integration has to be performed at each value of z_w. Each integration involves quite a few number of simulations at high temperatures, where the properties of clusters are not of direct interest. The disadvantage is prominent when $N_i=N_a^c$, where the bisulfate-hydronium ion pairs form a cluster even above 2000 K. These unphysical states, nonetheless, have to be simulated if one uses Eq. (B1). It is more convenient to take an alternative integration path:

$$\Xi_w^c(\beta,V,\mu_w,N_a^c,N_i)$$

$$= \Xi_w(\beta_0,V,\mu_{w0},N_a^c,N_i)\exp\left[-\int_{\beta_0}^{\beta}\langle U_N\rangle_{z_{w0}}d\beta\right.$$

$$\left.+\int_{\log z_{w0}}^{\log z_w}\langle N_w\rangle_\beta d\log z_w\right], \tag{B2}$$

where, for an appropriate choice of β_0 in accordance with the ideal gas state just mentioned, $\Xi_w(\beta_0,V,\mu_{w0},N_a^c,N_i)$ is given by

$$\Xi_w(\beta_0,V,\mu_{w0},N_a^c,N_i)$$

$$= N_i!(V\Omega)^{N_a^c}e^{z_{w0}V\Omega}\left[\int d1\,e^{-\beta_0 u_{hb}(1)}\right]^{N_i}, \tag{B3}$$

where $N_i!$ accounts for the possible number of ways of forming the ion pairs from the ions which are regarded as distinguishable in $\Xi_w(\beta_0,V,z_{w0},N_a^c,N_i)$. In applying Eq. (B2), the temperature integration involving unphysical high temperature states has to be performed only once at fugacity z_{w0}. Unlike Eq. (B1), all the intermediate states between z_{w0} and z_w, as implied in the second integration in Eq. (B2), are of direct interest to us. In Appendix D, we introduce an approximation that further reduces the computational effort.

It is convenient to rewrite Eq. (B2) in terms of excess quantities. For this purpose, we rewrite the factors involving z_{w0} and β_0 in Eq. (B3) by means of the follow identities:

$$e^{z_{w0}\Omega V}=e^{n_{w0}V}=\exp\left[n_wV-\int_{\log n_{w0}}^{\log n_w}n_wVd\log n_w\right] \tag{B4}$$

and

$$\int d1\,e^{-\beta u_{hb}(1)}=\exp\left[-\int_{\beta_0}^{\beta}\langle u_{hb}\rangle d\beta\right]\int d1\,e^{-\beta_0 u_{hb}(1)}, \tag{B5}$$

where the thermal average is taken in the canonical ensemble of a single bisulfate-hydronium ion pair. Using Eqs. (B4) and (B5) in Eq. (B3) and substituting the resulting expression in Eq. (B2), we obtain

$$\Xi_w^c(\beta,V,\mu_w,N_a^c,N_i)$$

$$= N_i!(V\Omega)^{N_a^c}e^{n_wV}\left[\int d1\,e^{-\beta u_{hb}(1)}\right]^{N_i}$$

$$\times\exp\left\{-\int_{\beta_0}^{\beta}[\langle U_N\rangle_{n_{w0}}-N_i\langle u_{hb}\rangle]d\beta\right.$$

$$\left.+\int_{\log n_{w0}}^{\log n_w}[\langle N_w\rangle_\beta-n_wV]d\log n_w\right\}. \tag{B6}$$

At β_0, non-negligible interaction energies arise only from the ionic interaction in each of the ion pairs. Thus, the first integral in the exponential is independent of β_0 as long as it is chosen sufficiently small. The integrand in the second integral is the excess number of water molecules over the ideal gas value. Hence the integral is independent of V, provided that the system boundary is far from the molecules in the cluster. The volume dependence of the first integral is addressed in Appendix C.

TABLE X. Consistency check by means of Eq. (B7).

N_a^c	N_i	lhs of Eq. (B7)[a]	rhs of Eq. (B7)[a,b]
1	0	-15.96 ± 0.47	-15.58 ± 0.53
0	1	-61.21 ± 1.01	-60.42 ± 1.24
2	0	-39.91 ± 0.74	-39.79 ± 0.88

[a]Evaluated at $T=298.15$ K and $n_w=0.6\times10^{-6}$ Å^{-3}. In k_BT unit.
[b]$n_{w0}=0.1048\times10^{-6}$ Å^{-3}.

For an accurate estimate of the free energy, each thermal average in Eq. (B6) has to be evaluated at a sufficient number of points along the integration path. One way to verify if this condition is met is through the identity:

$$\int_{\beta_0}^{\beta}[\langle U_N\rangle_{n_w}-N_i\langle u_{hb}\rangle]d\beta$$

$$=\int_{\beta_0}^{\beta}[\langle U_N\rangle_{n_{w0}}-N_i\langle u_{hb}\rangle]d\beta$$

$$-\int_{\log n_{w0}}^{\log n_w}[\langle N_w\rangle_\beta-n_wV]d\log n_w, \tag{B7}$$

which follows from Eqs. (B1), (B2), and (B3). The identity Eq. (B7) is checked for a few cases and the results are shown in Table X. Within the range of the error bars, the agreement is excellent, indicating that the numbers of the intermediate temperatures, n_w, and the Monte Carlo steps in each simulation are sufficient.

APPENDIX C: CHOICE OF V

Equation (2) shows that $e^{-\beta W^{rev}}$ is the probability of finding a cluster in the system of volume V relative to the probability of finding no cluster. Since the cluster can be found anywhere in the system and the event of finding it at one place or another is mutually exclusive by our choice of V as discussed in Sec. III, we have

$$e^{-\beta W^{rev}}\sim V, \tag{C1}$$

provided that care is taken to avoid the surface effect of the system boundary. One way to achieve this is to fix one of the acid molecules at the center of the system and take the system boundary far from the molecules forming the cluster, which imposes a lower limit on V. Analytically integrating over the coordinates of the acid molecule thus fixed by ignoring the surface effect, we obtain Eq. (C1).

The upper limit on V arises from the condition Eq. (16) and the requirement that Ξ_w^c be evaluated accurately by simulation of a finite length of time. Combining Eqs. (2), (3), (7), (10), and (C1), we obtain

$$\Xi_w^c\sim Ve^{n_wV}. \tag{C2}$$

Using Eq. (C2) in Eq. (B6), we find that

$$-\int_{\beta_0}^{\beta}[\langle U_N\rangle_{n_{w0}}-N_i\langle u_{hb}\rangle]d\beta=(1-N_a^c)\log V+\text{const.} \tag{C3}$$

When the left-hand side (lhs) of Eq. (C3) is evaluated from a simulation, one can address its accuracy by examining if Eq.

TABLE XI. Proportionality constant of log V in Eq. (C3).

N_a^c	N_i	Simulation	Eq. (C3)
2	1	-1.04 ± 0.14	-1
2	0	-0.93 ± 0.03	-1
3	0	-1.94 ± 0.07	-2

(C3) is satisfied. Note that, at β, the probability for N_a^c acid molecules to form a single cluster with water molecules must be dominant, namely, the cluster is stable with respect to evaporation of acid molecules. On the other hand, at β_0, the probability that they form an ideal gas is dominant. Around the temperature range where the acid molecules start to evaporate, both ideal gas vapor and the cluster have comparable probabilities. Thus, for the thermal averages to be estimated correctly in this temperature range, the probability for molecules to collide has to be non-negligible even after an evaporation event. Since simulation can be performed only for a finite period of time, V must be chosen to be sufficiently small, which imposes an upper limit on V. In particular, we choose V so that Eq. (C3) holds for a certain range of V including the one employed in simulation.

Note that the last integrand in Eq. (B6) is the excess number of water molecules over the ideal gas value resulting from the presence of the cluster and is independent of V if it is larger than its lower limit mentioned above. Thus, its integral is absorbed in the constant term. The particular form of V dependence shown in Eq. (C3) is not surprising since the integral in the equation is the reversible work required to form a cluster from the ideal gas state by gradually turning on the interaction among water and acid molecules and hence reflects the change in the entropic contributions of the acid molecules. Such terms as $\langle N_w \rangle \log V$ do not arise in Eq. (C3), since the system is open to water molecules.

To verify that our choice of V satisfies Eq. (C3), we calculated the lhs of the equation for four different values of V corresponding to the container radius of 25, 37.5, 50, and 64 Å. Since Eq. (C3) is concerned with the change in entropic contributions of acid molecules, simulation was performed in the canonical ensemble in the absence of water molecules for 3×10^8 MC steps. The temperature corresponding to the upper limit of the integral in Eq. (C3) is 400 K since, as the acid molecules form a cluster below this temperature, the integrand in Eq. (C3) becomes independent of V, thereby contributing to the constant term in Eq. (C3). Also, in the temperature range involved, $\langle N_w \rangle$ is negligible, again verifying the use of the canonical ensemble. The resulting values of the lhs of Eq. (C3) were least-squares fitted to a linear equation. The value of the proportionality constant of log V is compared with the theoretical one, $1 - N_a^c$, in Table XI, revealing nearly exact agreement. Thus, our choice of V, corresponding to the container radius of 50 Å, is appropriate in view of the number of MC steps involved in simulation.

In cluster simulation in a canonical ensemble, a system is commonly taken as a spherical container concentric with the center of mass of molecules forming a cluster. Then, one chooses V so that thermodynamic properties of a cluster are insensitive to the exact choice of V. Since the center of mass of the cluster is fixed in this case, thermodynamic properties of the cluster evaluated from simulation reflect only the internal degrees of freedom of the cluster. It follows that if such choice of V is in fact possible, the cluster possesses a well-defined translational degrees of freedom as a whole when it is placed in the vapor phase, and *vice versa*. This, in turn, is necessary for nucleation theory to be formulated in terms of the concept of cluster as in the classical theory. Under an idealized circumstance where simulation can be performed for an indefinite period of time, Eq. (C3) can be interpreted as a necessary and sufficient condition for a cluster to possess a well-defined translational degrees of freedom as a whole. This indicates that Eq. (C3), when applied to canonical ensemble cluster simulation, is an explicit implementation of the criterion by Lee *et al.*[34] in choosing V.

APPENDIX D: THE FUGACITY DEPENDENCE OF W^{rev}

In this work, independent simulations were performed at several values of the fugacity z_w of water. Under a certain reasonable approximation, however, the results obtained at fugacity z_w can be used to estimate W^{rev} at different fugacity z_w'. Since this offers an improvement of the computational efficiency by a factor of several, we shall briefly describe the method here.

The time scale for a cluster to reach the internal mechanical equilibrium is many orders of magnitude shorter than that for the cluster to exchange a molecule with the vapor phase. Therefore, it is a common practice to assume that the configurational integral of an (N_a^c, N_w^c) cluster is independent of the fugacity. Under this assumption, the first equality of Eq. (19) yields

$$\Xi^c(\beta, V, \mu_w', \mu_s; N_a^c, N_w^c)$$

$$= e^{n_s V} \left(\frac{q_s e^{\beta \mu_s}}{\Lambda_s^3} \right)^{N_a^c} \sum_{N_i=0}^{N_a^c} \frac{\chi^{N_i}}{(N_a^c - N_i)! N_i!} \frac{z_w'^{N_i}}{N_i!} \frac{z_w'^{N_w}}{N_w!}$$

$$\times \int d\{N\} e^{-\beta U_N}$$

$$= e^{n_s V} \left(\frac{q_s e^{\beta \mu_s}}{\Lambda_s^3} \right)^{N_a^c} \sum_{N_i=0}^{N_a^c} \frac{\chi^{N_i}}{(N_a^c - N_i)! N_i!} \left(\frac{z_w'}{z_w} \right)^{N_w^c} \frac{z_w^{N_i}}{N_i!} \frac{z_w^{N_w}}{N_w!}$$

$$\times \int d\{N\} e^{-\beta U_N}. \tag{D1}$$

Since Eq. (D1) differs from Eq. (19) only by the factor of $(z_w'/z_w)^{N_w^c}$, the desired expression for the reversible work follows from Eq. (21):

$$e^{-\beta W^{rev}(\beta, V, \mu_w', \mu_s; N_a^c, N_w^c)}$$

$$= (n_s V)^{N_a^c} \sum_{N_i=0}^{N_a^c} \left(\frac{z_w'}{z_w} \right)^{N_w^c} e^{-\beta \phi(\beta, V, \mu_w, N_a^c, N_i)}$$

$$\times p(\beta, V, \mu_w, N_a^c, N_i, N_w^c - N_i). \tag{D2}$$

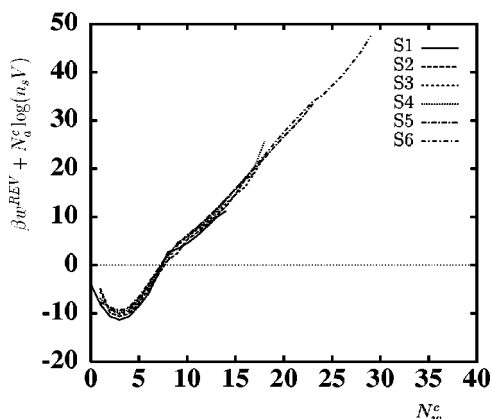The reversible work of the N_a^c cluster is obtained by taking a summation of Eq. (D2) with respect to N_w^c. For a direct

FIG. 20. Comparison of the reversible work of cluster formation for $N_a^c = 1$ at $T = 298.15$ K and $n_w = 0.1 \times 10^{-6}$ Å^{-3} obtained through Eq. (D2) by using other values of n_w. The conditions of simulation for S1, ... ,S6 are given in Table VIII. $f_{hb} = 20$ kcal/mol.

application of Eq. (D2) to yield the reversible work of cluster formation at z_w' of interest, it is necessary that the range over which $p(\mu_w, N_w)$ is non-negligible and that for $p(\mu_w', N_w)$ overlap in a wide range of N_w. One can easily circumvent this condition by means of the umbrella sampling, which was employed in the free energy evaluation for a homogeneous nucleation in a single component system.[95]

To demonstrate the utility of Eq. (D2), we calculated W^{rev} at $n_w' = 0.1 \times 10^{-6}$ Å, using the result of the simulations performed at the other values of n_w as summarized in Table VIII. The result is shown in Fig. 20, which indicates a remarkable agreement of the calculated values of W^{rev}. The slight discrepancy arises because of the vapor contribution[95] to N_w^c and the change in the dominant part of p as n_w changes.

[1] H. Reiss, J. Chem. Phys. **18**, 840 (1950).
[2] D. Stauffer, J. Aerosol Sci. **7**, 319 (1976).
[3] V. A. Shneidman and M. C. Weinberg, J. Chem. Phys. **97**, 3621 (1992).
[4] V. A. Shneidman and M. C. Weinberg, J. Chem. Phys. **97**, 3629 (1992).
[5] L. M. Berezhkovskii and V. Yu. Zitserman, J. Chem. Phys. **102**, 3331 (1995).
[6] Z. Kožíšek and P. Demo, J. Chem. Phys. **102**, 7595 (1995).
[7] B. E. Wyslouzil and G. Wilemski, J. Chem. Phys. **103**, 1137 (1995).
[8] *Nucleation*, edited by A. C. Zettlemoyer (Marcel Dekker, New York, 1969).
[9] G. S. Springer, Adv. Heat Transfer **14**, 281 (1978).
[10] D. W. Oxtoby, J. Phys.: Condens. Matter **4**, 7627 (1992).
[11] G. J. Doyle, J. Chem. Phys. **35**, 795 (1961).
[12] P. Mirabel and J. L. Katz, J. Chem. Phys. **60**, 1138 (1974).
[13] P. Mirabel and J. L. Ponche, Chem. Phys. Lett. **183**, 21 (1991).
[14] R. H. Heist and H. Reiss, J. Chem. Phys. **61**, 573 (1974).
[15] W. J. Shugard, R. H. Heist, and H. Reiss, J. Chem. Phys. **61**, 5298 (1974).
[16] W. J. Shugard and H. Reiss, J. Chem. Phys. **65**, 2827 (1976).
[17] F. J. Schelling and H. Reiss, J. Chem. Phys. **74**, 3527 (1981).
[18] A. Jaecker-Voirol, P. Mirabel, and H. Reiss, J. Chem. Phys. **87**, 4849 (1987).
[19] A. Jaecker-Voirol and P. Mirabel, J. Phys. Chem. **92**, 3518 (1988).
[20] A. Jaecker-Voirol and P. Mirabel, Atmos. Environ. **23**, 2053 (1989).
[21] M. Kulmala and A. Laaksonen, J. Chem. Phys. **93**, 696 (1990).
[22] M. Kulmala, M. Lazaridis, A. Laaksonen, and T. Vesala, J. Chem. Phys. **94**, 7411 (1991).
[23] A. Laaksonen and M. Kulmala, J. Am. Med. Assoc. **22**, 779 (1991).
[24] M. Lazaridis, M. Kulmala, and A. Laaksonen, J. Aerosol Sci. **22**, 823 (1991).
[25] K. Nishioka and K. Fujita, J. Chem. Phys. **100**, 532 (1994).
[26] R. McGraw, J. Chem. Phys. **102**, 2098 (1995).
[27] H. Reiss, D. I. Margolese, and F. J. Schelling, J. Colloid Interface Sci. **56**, 511 (1976).
[28] D. Boulaud, G. Madelaine, D. Vigla, and J. Bricard, J. Chem. Phys. **66**, 4854 (1977).
[29] P. Mirabel and J. L. Clavelin, J. Chem. Phys. **68**, 5020 (1978).
[30] F. J. Schelling and H. Reiss, J. Colloid Interface Sci. **83**, 246 (1981).
[31] B. E. Wyslouzil, J. H. Seinfeld, R. C. Flagan, and K. Okuyama, J. Chem. Phys. **94**, 6842 (1991).
[32] Y. Viisanen, M. Kulmala, and A. Laaksonen, J. Chem. Phys. **107**, 920 (1997).
[33] M. P. Allen and D. J. Tildesley, *Computer Simulation of Liquids* (Oxford University Press, New York, 1987).
[34] J. K. Lee, J. A. Barker, and F. F. Abraham, J. Chem. Phys. **58**, 3166 (1973).
[35] H. Reiss, A. Tabazadeh, and J. Talbot, J. Chem. Phys. **92**, 1266 (1990).
[36] H. M. Ellerby, C. L. Weakliem, and H. Reiss, J. Chem. Phys. **95**, 9209 (1991).
[37] H. M. Ellerby and H. Reiss, J. Chem. Phys. **97**, 5766 (1992).
[38] C. L. Weakliem and H. Reiss, J. Chem. Phys. **99**, 5374 (1993).
[39] C. L. Weakliem and H. Reiss, J. Chem. Phys. **101**, 2398 (1994).
[40] K. J. Oh, X. C. Zeng, and H. Reiss, J. Chem. Phys. **107**, 1242 (1997).
[41] D. I. Zhukhovitskii, J. Chem. Phys. **103**, 9401 (1995).
[42] R. Evans, Adv. Phys. **28**, 143 (1979).
[43] D. W. Oxtoby and R. Evans, J. Chem. Phys. **89**, 7521 (1988).
[44] X. C. Zeng and D. W. Oxtoby, J. Chem. Phys. **94**, 4472 (1991).
[45] X. C. Zeng and D. W. Oxtoby, J. Chem. Phys. **95**, 5940 (1991).
[46] V. Talanquer and D. W. Oxtoby, J. Chem. Phys. **99**, 4670 (1993).
[47] V. Talanquer and D. W. Oxtoby, J. Chem. Phys. **102**, 2156 (1995).
[48] V. Talanquer and D. W. Oxtoby, J. Chem. Phys. **103**, 3686 (1995).
[49] V. Talanquer and D. W. Oxtoby, J. Phys. Chem. **99**, 2865 (1995).
[50] D. W. Oxtoby, V. Talanquer, and A. Laaksonen, in *Nucleation and Atmospheric Aerosols*, Proceedings of the 14th International Conference on Nucleation and Atmospheric Aerosols, edited by M. Kulmala and P. E. Wagner (Pergamon, New York, 1996), pp. 21–29.
[51] I. Kusaka, Z.-G. Wang, and J. H. Seinfeld, J. Chem. Phys. **102**, 913 (1995).
[52] I. Kusaka, Z.-G. Wang, and J. H. Seinfeld, J. Chem. Phys. **103**, 8993 (1995).
[53] V. Talanquer and D. W. Oxtoby, J. Chem. Phys. **106**, 3673 (1997).
[54] E. Kochanski *et al.*, J. Chim. Phys. Phys.-Chim. Biol. **88**, 2451 (1991).
[55] R. Kelterbaum, N. Turki, A. Rahmouni, and E. Kochanski, J. Mol. Struct.: THEOCHEM **314**, 191 (1994).
[56] R. L. Kuczkowski, R. D. Suenram, and F. J. Lovas, J. Am. Chem. Soc. **103**, 2561 (1981).
[57] J. W. Gibbs, *The Scientific Papers of J. Willard Gibbs* (Dover, New York, 1961), Vol. I.
[58] I. Kusaka, Z.-G. Wang, and J. H. Seinfeld, Presented at the 14th International Conference on Nucleation and Atmospheric Aerosols in Helsinki, 1996.
[59] H. J. C. Berendsen, J. R. Grigera, and T. P. Straatsma, J. Phys. Chem. **91**, 6269 (1987).
[60] W. R. Cannon, B. M. Pettitt, and J. A. McCammon, J. Phys. Chem. **98**, 6225 (1994).
[61] A. Loewenstein and A. Szöke, J. Am. Chem. Soc. **84**, 1151 (1962).
[62] Z. Luz and S. Meiboom, J. Am. Chem. Soc. **86**, 4768 (1964).
[63] B. N. Hale and S. M. Kathmann, in Ref. 50, pp. 30–33.
[64] T. H. Lay (private communication).
[65] F. H. Stillinger and C. W. David, J. Chem. Phys. **69**, 1473 (1978).
[66] J. W. Halley, J. R. Rustad, and A. Rahman, J. Chem. Phys. **98**, 4110 (1993).
[67] L. Kurdi and E. Kochanski, Chem. Phys. Lett. **158**, 111 (1989).
[68] D. K. Remler and P. A. Madden, Mol. Phys. **70**, 921 (1990).
[69] K. Laasonen, M. Sprik, M. Parrinello, and R. Car, J. Chem. Phys. **99**, 9080 (1993).
[70] M. Tuckerman, K. Laasonen, M. Sprik, and M. Parrinello, J. Phys. Chem. **99**, 5749 (1995).
[71] M. Tuckerman, K. Laasonen, M. Sprik, and M. Parrinello, J. Chem. Phys. **103**, 150 (1995).
[72] R. G. Parr and W. Yang, *Density-Functional Theory of Atoms and Molecules* (Oxford University Press, New York, 1989).
[73] Y. K. Lau, S. Ikuta, and P. Kebarle, J. Am. Chem. Soc. **104**, 1462 (1982).
[74] X. Yang and A. W. Castleman, Jr., J. Am. Chem. Soc. **111**, 6845 (1989).
[75] X. Yang and A. W. Castleman, Jr., J. Geophys. Res. **96**, 22573 (1991).

[76] Z. Shi, J. V. Ford, S. Wei, and A. W. Castleman, Jr., J. Chem. Phys. **99**, 8009 (1993).

[77] M. D. Newton, J. Chem. Phys. **67**, 5535 (1977).

[78] C. K. Lutrus, D. E. Hagen, and S. H. S. Salk, Atmos. Environ., Part A **24A**, 1397 (1990).

[79] M. W. Jurema, K. N. Kirschner, and G. C. Shields, J. Comput. Chem. **14**, 1326 (1993).

[80] A. Khan, Chem. Phys. Lett. **217**, 443 (1994).

[81] R. Kelterbaum and E. Kochanski, J. Phys. Chem. **99**, 12493 (1995).

[82] Y. Guissani and B. Guillot, J. Chem. Phys. **98**, 8221 (1993).

[83] J. Alejandre, D. J. Tildesley, and G. A. Chapela, J. Chem. Phys. **102**, 4574 (1995).

[84] R. S. Taylor, L. X. Dang, and B. C. Garrett, J. Phys. Chem. **100**, 11720 (1996).

[85] E. Kochanski, J. Chim. Phys. Phys.-Chim. Biol. **8**, 605 (1984).

[86] S. L. Fornili, M. Migliore, and M. A. Palazzo, Chem. Phys. Lett. **125**, 419 (1986).

[87] Y. Guissani, B. Guillot, and S. Bratos, J. Chem. Phys. **88**, 5850 (1988).

[88] R. E. Kozack and P. C. Jordan, J. Chem. Phys. **96**, 3131 (1992).

[89] W. R. Rodwell and L. Radom, J. Am. Chem. Soc. **103**, 2865 (1981).

[90] K. Morokuma and C. Muguruma, J. Am. Chem. Soc. **116**, 10316 (1994).

[91] W. Studziński, G. H. Spiegel, and R. A. Zahoransky, J. Chem. Phys. **84**, 4008 (1986).

[92] J. L. Katz, H. Saltsburg, and H. Reiss, J. Colloid Interface Sci. **21**, 560 (1966).

[93] K. Nishioka and G. M. Pound, Adv. Colloid Interface Sci. **7**, 205 (1977).

[94] R. Kubo, *Statistical Mechanics* (Elsevier, Amsterdam, 1965).

[95] I. Kusaka, Z.-G. Wang, and J. H. Seinfeld, J. Chem. Phys. **108**, 3416 (1998).

[96] S. Tabata, J. Appl. Meteorol. **12**, 1410 (1973).

[97] Pictures of clusters were produced by a program RASMOL developed by Dr. R. Sayle.

[98] H. Resat and M. Mezei, Biophys. J. **71**, 1179 (1996).

[99] Thermodynamic data necessary in classical theory are obtained from the program kindly provided to us by Dr. Markku Kulmala.

[100] D. Kashchiev, J. Chem. Phys. **76**, 5098 (1982).

[101] Y. Viisanen, R. Strey, and H. Reiss, J. Chem. Phys. **99**, 4680 (1993).

[102] R. Strey and Y. Viisanen, J. Chem. Phys. **99**, 4693 (1993).

[103] D. W. Oxtoby and D. Kashchiev, J. Chem. Phys. **100**, 7665 (1994).

[104] H. B. Callen, *Thermodynamics and an Introduction to Thermostatistics*, 2nd ed. (Wiley, New York, 1985).

[105] I. Prigogine and R. Defay, *Chemical Thermodynamics* (Longmans, London, 1954), translated by D. H. Everett.

[106] S. G. Lias *et al.*, J. Phys. Chem. Ref. Data Suppl. 1 **17**, 1 (1988).